Modeling the growth and regional extent of new particle formation events

2013-08-30

Bachelor Thesis Summer 2013

Jimmie Carpman

Supervisors: Niku Kivekäs

Adam Kristensson

LUND UNIVERSITY

Abstract

As aerosol particles are important for global climate effects, their sources and influence on global aerosol particle concentrations need to be quantified. One of the major aerosol sources in the atmosphere is new particle formation (NPF) of new nanometer sized particles in the atmosphere. The influence on the global aerosol concentration due to NPF events is however not well quantified. The goals of this study is to examine how new particle formation (NPF) events influence the regional particle number size distribution in the air and how this affect the time dependent number size distribution measured at different field sites around the world. The method we used to approach this was to create a one dimensional box model including various aerosol dynamic processes that simulates NPF events during long range transport in the atmosphere. The factors, which influence NPF events and the resulting size distributions that can be studied in this model are: 1. Particle formation rates during NPF events. 2. Wind speed, and 3. Growth of the newly formed particles.

In the examination of the effects of the aerosol dynamic processes, coagulation and dry deposition, the analysis showed us the effectiveness of coagulation in removing small particles (< 10 nm diameter) and that dry deposition was also effective in removing the largest particles below 1 μm diameter.

During the examination of the effect of formation rates, we could clearly see that the concentration of particles is dependent on the magnitude of the NPF event. If the formation takes place over a smaller geographical area the NPF events, as registered at a downwind site, were consisting of particles of approximately the same size.

During the simulations with varying time and place where particles experienced growth during NPF events, the size distribution measured downwind of where the particles were formed showed relatively varying sizes and concentrations, which is difficult to interpret in real situations at a field site where the size distribution is measured. With this model, these situations can be understood and simulated.

We have, however, not tried the model against measured data at field sites. In future research one should include quantifying the effects at field sites and continue to investigate in detail the other effects of varying different factors like the wind speed, formation rate and growth rate during NPF events.

Table of contents

1. Introduction

The aerosol particles play an important role in the Earth's atmosphere. Aerosol particles influence the climate by altering the radiation balance by their direct and indirect effects. The particles influence the radiation balance directly through scattering and absorption of incoming sunlight, where the scattering has a reducing effect on heating the earth surface and biosphere, while the absorption increase the temperature in the atmospheric layer where the particles are located. The particles influence the radiation balance also indirectly by acting as cloud condensation nuclei (CCN) for cloud droplets, which absorb outgoing infrared radiation from the surface of the earth and are very effective at scattering the incoming solar radiation. To understand how the aerosol particles influence the climate, detailed information is needed on how different aerosol sources affect the atmospheric particle population, and how the aerosol particles are transformed in the atmosphere. One of the most important particle sources is new particle formation (NPF), where new particles are formed from gaseous precursors in the atmosphere. These new nanometer sized particles can be formed in different ways; through homogeneous nucleation involving only gas-phase species in the formation or heterogeneous nucleation, which involves the interaction of gas molecules with already existing nanometer sized particle clusters of a different chemical composition than the molecules.

The magnitude of the indirect climate effect due to NPF is different depending on where in the atmosphere the NPF takes place. A global model estimate shows that the contribution to CCN formation from NPF is as high as 45% from which 35% of the CCN come from NPF in the free troposphere and 10% from the boundary layer. (Merikanto et al., 2009). The NPF contribution to CCN in low-level clouds is bigger over marine regions (55%) compared to over land areas (33%), since the fraction of CCN that come from other sources than NPF are much higher over the continents than over the sea. But even in the worst polluted continental areas, like South-East Asia, the contribution of NPF on CCN is as high as 19%. There are however large uncertainties in these estimates, and one source of uncertainty is the use of constant formation and growth rates during NPF. While formation and growth rates during NPF are not constant as function of time and place in the atmosphere, the use of constant values has been justified in the global models due to the poor understanding of these factors. (Merikanto et al., 2009).

Even though regional new particle formation has been observed around the world (Kulmala et al., 2004 and references therein), the regional assumptions are typically based on what we observe at a single measurement site. There have been only a few studies addressing the regional extent of the same events at multiple sites (Komppula et al., 2006; Hussein et al., 2009; Väänänen et al., 2013).

To be able to understand in a better way how formation and growth rates vary as function of time and space, we created and run a model that artificially simulates the effect of varying formation and growth rates during NPF.

2. Theory

2.1. Aerosols and aerosol processes

2.1.1. Aerosol sources

The atmospheric aerosol particle sources can be separated into two groups. Primary particles which are produced directly at the source and secondary particles which are created by gas-to-particle conversion in the atmosphere. In real life it is often hard to attribute a particle population to a specific primary or secondary source. For example, if the particles have been formed as 20 nm diameter organic particles in a city from car engine exhaust, but have grown due to condensation of sulfuric acid during atmospheric transport to sizes around 40 nm diameters 1 day after the city emissions, then their origin is hard to deduce. By measuring these 40 nm particles containing both sulfuric acid and organic compounds, it is not straightforward to know what has been their fate during their lifetime, and what their source of the sulfuric and organic content is.

- Primary particles

  The primary particles can be emitted through combustion, by mechanical generation or from biological sources.

  The important combustion sources are vehicle engine combustion, forest fires, coal power plant combustion, biomass combustion and volcanoes.

  The mechanically generated particles have their source from windblown soil dust and desert sand, wave-breaking and mechanical grinding. With the windblown sources we mean that the wind acts on a dry surface so the particles are lifted from the surface and by that process become airborne in the atmosphere. Wave-breaking particles are produced during wave's surges over the sea areas, which lead to the atmospheric emission of small droplets. Once these have become airborne, the water evaporates from them, and only the salt and organic matter remains in the aerosol particle. One very important atmospheric mechanically grinded particle type is the one produced through the contact with car tires and the road surface. The wearing down of the asphalt by the tires, and the wearing down of tire and brake material creates a road surface deposit of particles. As the road surface becomes dry, these deposited particles have a chance to become airborne through the wind acting on the road surface or through the turbulence generated by the moving vehicles. Another source of mechanically grinded particles is construction activity and stone-crushing in gravel production.

  Finally the important biological particles are pollen, bacteria, fungal, spores, viruses, algae and biological crusts.

- Secondary particles

  The source types of secondary particles are belonging to two different groups in particular, condensation of gases on already existing particles and new particle formation (NPF), which is the formation of new particles from gaseous precursors.

Condensation does only influence the mass concentration of the particles in the atmosphere but the new particle formation influences both mass concentration and number concentration. These particles are, however, so small that the direct contribution of NPF to mass concentration can be neglected.

Condensation will be discussed in more detail in chapter 2.1.5 and new particle formation will be discussed more in the next chapter.

2.1.2. New particle formation (NPF)

New particle formation (NPF) leads to frequent formation of new particles in the atmosphere between 1 and 2 nm diameter in size (Kulmala et al., 2013). The formation can occur in two different ways:

1. Homogeneous formation: As gas molecules are merged together, they form a new nanometer sized particle. This type of formation occurs without involving any foreign particles or surfaces.

2. Heterogeneous formation: This is nucleation when gas molecules interact with an already existing neutral cluster or ion cluster. During the interaction, the cluster becomes activated and turns into a slightly larger and stable nanometer sized particles.

Places with frequent observations of new particle formation events is in the free atmosphere, the boreal forest, Eastern United States, Germany, other places in Europe, Coastal environments in Europe and USA (Kulmala et al., 2004). There have also been observations in almost every environment in the world from the polar regions (eg. Kyrö et al., 2013) to the deep jungles (eg. Krejci et al., 2005) but there are few measurements in these regions.

Much of the NPF takes place on sunny, clear days according to Kulmala et al. 2004, and usually on one occasion during the day, around or before noon. These formation bursts are referred to as NPF events. According to measurements the nucleation events often show a common smooth growth to sizes of several tens of nanometer in diameter due to condensation. If the growth can be followed during many hours, it proves that an NPF event has a regional extent of several hundreds of kilometers (Hussein et al., 2009), and can also contribute to cloud droplet activation (Kerminen et al., 2005). An example of an NPF event can be seen from the Vavihill background field station, located in southern Sweden, (Johansson et al., 2011) in figure 1. The newly formed mode of particles around 3 nm diameter is growing due to condensation to sizes around 30 nm diameter at the end of the day as can be seen in the one diurnal time plot of the size distribution in figure 1. This growth appears as a “banana” in the plot.

It is not until in recent years that the instrument development has given the opportunity to measure the concentration and chemical composition of particles smaller than the earlier 3 nm diameter limit, and therefore our understanding of mechanisms, vapors and clusters involved in the particle formation remains an open issue (Kulmala et al., 2013).

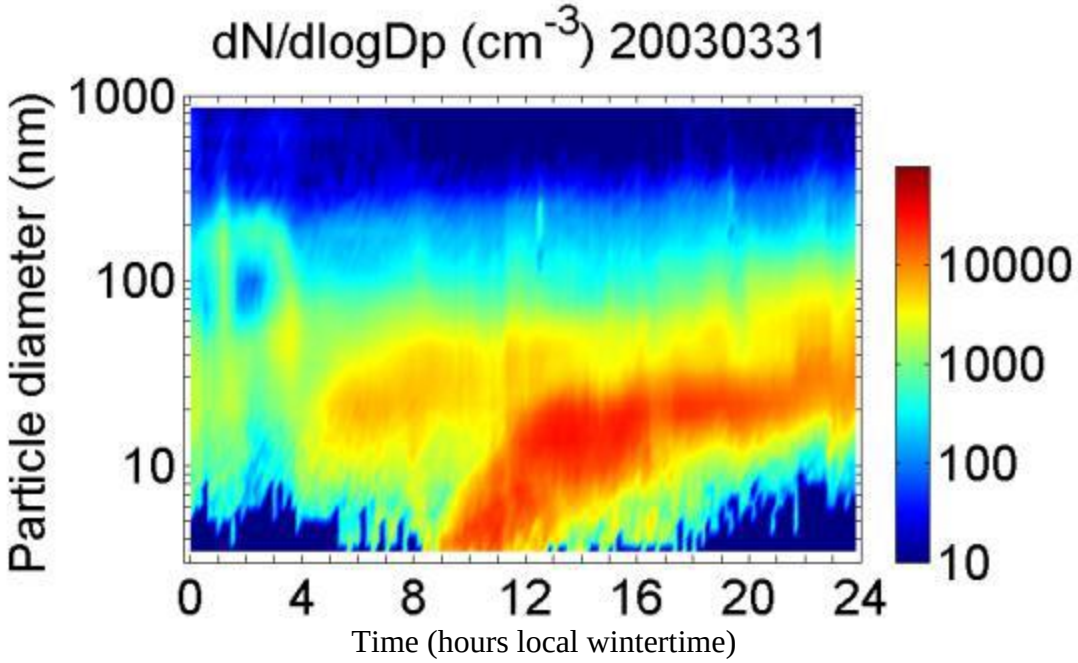

Figure 1: The particle number size distribution measured at the Vavihill field site during March 31, 2003 (Johansson et al., 2011).

2.1.3. Particle number size distribution in the atmosphere

In the atmosphere we have aerosols in a wide spread size range, from as small as 1 nanometer to a size of several hundred micrometers. All these particles are then divided into four different size classes called modes. The modes are the nucleation mode up to 30 nm, Aitken mode from 30 nm to 100 nm, accumulation mode from 0,1 µm to 1 µm and the coarse mode from 1 µm and bigger. The nucleation and Aitken modes often constitute the majority of all aerosols in the atmosphere by number but because the particles are so small they only account for just a few percent on the total mass of the aerosols. (Seinfeld and Pandis, 2006). The particles in the nucleation mode are formed in two different ways; first they are formed from condensation of hot vapors from combustion processes and secondly from nucleation (new particle formation) from trace species in the atmosphere but these particles quickly get removed by growing to bigger particles by coagulation with bigger particles and by the secondary process of condensation. The third mode is the accumulation mode which ranges from 0,1 µm to 1 µm. This mode accounts for a big amount of the aerosol mass and also the surface area of all aerosols. The accumulation mode has got its name because particles accumulate in this size ranges due to the removal mechanisms being weaker here compared to the other modes. Particles in the nucleation and Aitken modes grow through condensation and coagulation, and eventually reach this size mode. Finally there is the coarse mode that consists of all particles larger than 1 µm. These particles have their source from mechanical grinding from human activities and from natural sources like windblown dust. The removal processes of the course particle are very effective as the particles in the nucleation and Aitken mode, although different, so the lifetimes of these modes are much shorter than the lifetime of the accumulation mode.

2.1.4. Condensation

As a certain gas molecule experiences a vapor concentration (or vapor pressure) exceeding the saturation vapor pressure needed for the absorption of gas molecules to an aerosol particle, the gas molecule can condense on the aerosol particle surface. The saturation vapor pressure is different for different gases. The lower the value, the easier it is for the gas to reach the particle phase (Seinfeld and Pandis, 2006). Many different inorganic and organic compounds have a relatively low saturation vapor pressure needed for condensation. If the concentration of these vapors is high enough, the particles can grow rapidly due to the adsorption, increasing their mass concentration, and the particle alters chemical composition. The particle can contain thousands of compounds, which depend on the chemistry during the time when the particle was formed, and on which gases are condensing on the particle during long range transport in the atmosphere. Once the particles have grown to accumulation mode sizes due to condensation, further growth is not affecting the particle size any longer to a large extent, since these particles are already large, and the addition of compounds to the particle has a relatively small effect.

2.1.5. Coagulation

The particles within the aerosol collide with each other and during a collision they can undergo coalescence or aggregation. This will affect the number size distribution of the aerosol. The result will lead to the mode growing in size and the number concentration to decrease. (Hinds, 1999). The speed of the coagulation depends mainly on the number concentration and size of the particles. Smaller particles move faster and more randomly giving them a higher chance to collide with larger particles which have a larger inertia, and a larger surface area. (Hinds, 1998). In other words, this results in most numerous collisions between particles with large size difference.

Coagulation is most effective for removing small particles and therefore acts as a sink for small particles. (Kerminenet al., 2004; Seinfeld and Pandis, 2006).

2.1.6. Cloud processing and CCN

If the atmosphere was particle free it would need a relative humidity of several hundred percent to be able to form any water droplets. That is why particles in the atmosphere are essential. The activation in the presence of particles depends on the particle size, chemical and physical composition and the supersaturation of the air. The latter is defined as relative humidity – 100%. An activated particle can grow in size freely into a cloud droplet. Particles that can be activated by this process are defined as cloud condensation nuclei (CCN) for a given supersaturation they currently are experiencing. So, in order for clouds to be formed we need particles that can act as CCN and a relative humidity higher than 100 percent. (Seinfeld and Pandis, 2006).

Even when the relative humidity is less than 100 percent condensation of water on water soluble particles take place. The size of the droplet depends on the relative humidity and the droplet will shrink by evaporation if the relative humidity decreases and grow by condensation of water vapor if the relative humidity increases. (Frank, 2001).

During cloud processing by a cloud that does not rain out, the aerosol size and composition are changed by several different processes. First, some of the particles activate as CCN, so they grow to cloud droplets while the rest of the particles remain non-activated. This process

is called nucleation scavenging, and it defines the initial number concentration and composition of the cloud droplets. If no other process was taking place the aerosol distribution would go back to its original form after the cloud has evaporated. However, this is not the case. A numerous of other processes can modify the aerosol distribution, for instance collisions between the particles and droplets in the cloud, coalescence among the cloud droplets, or condensation of low vapor pressure gases on the droplets.

If the cloud produces rain, there are even more interactions that can occur between the particles and the raindrops both in the cloud and around it. This leads to a removal of particles in the atmosphere. There is also the possibility of NPF during evaporation of cloud droplets in the outflow of air from the clouds. (Seinfeld and Pandis, 2006).

2.1.7. Dry deposition

Deposition, both wet and dry, is the way in which particles are removed from the atmosphere.

Basically, dry deposition is the transport of gaseous and particulate species from the atmosphere to different surfaces without any precipitation. The elements that control the dry deposition of a particle are what physical and chemical properties they have, how the properties of the surface are and the amount of atmospheric turbulence. The turbulence, especially in the boundary layer, controls how much of the species that are delivered to the surface. The size, shape and density of a particle determine if it will get captured by the surface as the particles are in contact with the surface. The nature of the surface also plays a big role for the dry deposition, where higher and uneven obstacles will increase the deposition rate. Dry deposition is most effective for small and big particles. This relationship can be seen in figure 2 when looking at the line for the sum of all different deposition routes.

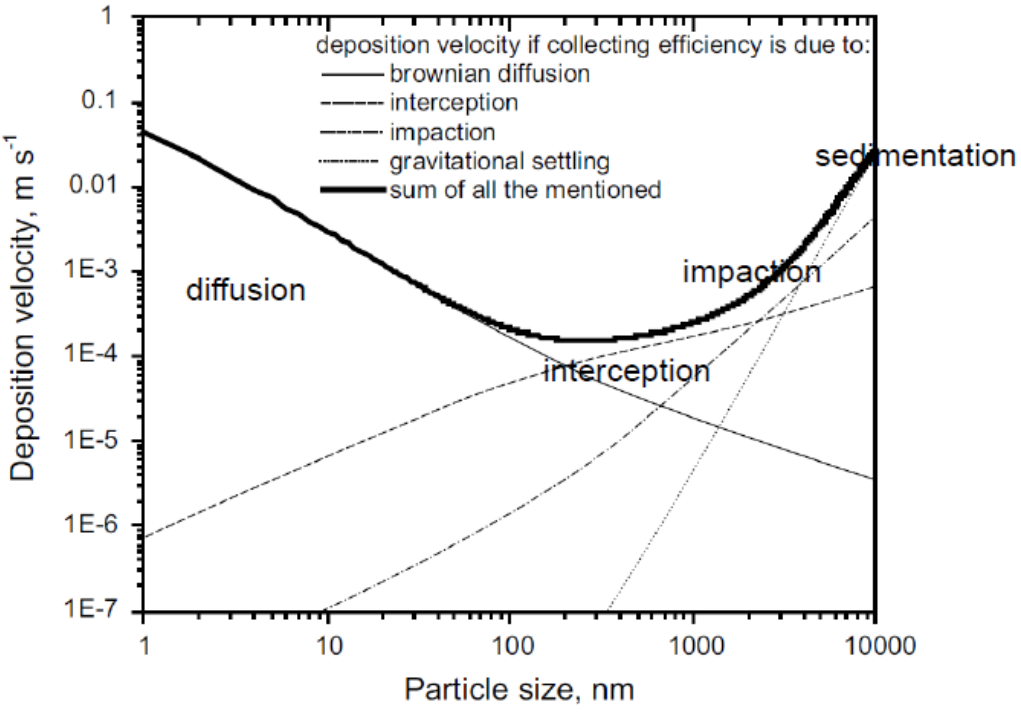

Figure 2: Dry deposition velocity as function of different deposition mechanisms depicted with thinner lines, and the total deposition rate indicated with the thick line. (Slinn, W. et al. 1982).

2.1.8. Wet deposition

Wet deposition is a process in which gases and particles are removed from the atmosphere by atmospheric hydrometeors. (cloud droplets, fog droplets, rain droplets, snow crystals etc.). There are different names for different deposition mechanisms. When aerosol particles are removed by raining clouds, it is called in-cloud scavenging, and it is called washout when aerosol particles are removed below clouds by the falling rain or snow. Wet removal, is a common name for all of these processes.

What is interesting with wet removal is that almost all processes are reversible until the particle is brought down to earth's surface. If particles form rain drops or snow flakes, the reverse of this process is evaporation of the droplets, which produces the new aerosol particles to be released again in the atmosphere.

2.1.9. Climate effects

There are two ways in which the aerosol particles can affect climate: Via 1. the direct effect, or via 2. the indirect effect.

The direct effect is when an increased amount of sunlight is absorbed or reflected by an increased concentration of aerosol particles. The change in the direct radiative forcing in the earth atmosphere from an increased aerosol particle concentration is measured in Wm^{-2}. The radiative forcing is the balance between incoming radiation and outgoing radiation of the earth's climate system. The reflected radiation depends on the optical properties, size and quantity of the aerosol particles and the solar zenith angel. The result of the direct climate effects is an increase of light reflected by the planet and by this a decrease of solar radiation that reaches the surface of the earth. So the direct effect cools the earth's surface temperature. (IPCC, 2012).

The indirect climate effects describe how aerosol particles act as cloud condensing nuclei (CCN), which alter cloud droplet properties and thereby the radiative properties of the clouds. The first indirect climate effect arises when anthropogenic sources increase the number concentration of CCN, which leads to a larger concentration of droplets with smaller radii giving a higher cloud albedo. The second indirect effect is when these droplets don't form rain drops as easily as larger ones, and therefore don't precipitate, thus increasing the life time of the cloud. The indirect effects are more complex and more difficult to determine than the direct effects because they depend on a chain of phenomena. If there is a change in aerosol levels, the concentration of cloud condensation nuclei changes which gives a change in cloud droplet number concentrations and also the size of them and these, in turn, are connected to the cloud albedo and the clouds lifetime. Other meteorological effects like changes in precipitation can also occur as a result of perturbations in the number concentration of aerosols. What complicates the picture further is the addition of gases and particles in the atmosphere that can even inhibit cloud formation, thereby giving a decreased cooling due to the indirect effect. (IPCC, 2012).

So the total effects of aerosols are hard to establish. Compared to the greenhouse gases which practically only act on the outgoing infrared radiation, the aerosol particles acts on both sides of the energy balance. The small particles, less than 1µm, are effective in scattering the solar radiation which cools the climate. Larger particles above 100 nm diameter and mainly soot

particles are good absorbers of sunlight so these particles have a warming effect on the climate. Mineral dust particles are good at both absorbing outgoing radiation and at scattering incoming radiation; however the mineral dust particles have an overall cooling effect. (Seinfeld and Pandis, 2006).

The greenhouse gases have lifetimes of several years or hundreds of years, and therefore have almost the same concentrations globally, whereas the aerosol concentration varies over time and space with lifetimes of days to weeks. Also the negative aerosol forcing occurs only on the daytime and the greenhouse gases forcing occur both day and night. When superimposed on each other the warming effects of greenhouse gases and the cooling effects of aerosols do not occur at the same locations. (Seinfeld and Pandis, 2006). The aerosol particles are the largest source of uncertainty of the radiative forcing among all atmospheric constituents. (IPCC, 2012).

2.2. Air transport and air mass trajectories

The main reason to use trajectories is in the use of forward trajectories in numerical weather forecast and in calculating where some known pollutants are transported. Another application is the use of back trajectories, where it is possible to investigate where the air comes from. For instance, back trajectories are used in studies to determine where the source of the pollutant air is coming from.

Atmospheric dispersion modeling is when you use numerical methods to compute the time evolution of an air mass. That is the way of calculating the backward trajectory of the air mass. This is normally divided into two categories. The Eulerian methods are used when the emission scenarios are very complex and not restricted to a limited number of grid points. The Lagrangian methods are used when there are single-point-source emissions and they are restricted to a few grid points and this model can be used with a higher spatial and time resolution than Eulerian models. (Draxler R.R. and Hess,G.D., 1998).

A widely used model to calculate trajectories is the Hybrid Single-Particle Lagrangian Integrated Trajectory (HYSPLIT) model. This model is a hybrid between the Eulerian and Lagrangian approaches. (Draxler, R.R., and G.D. Hess, 1998). There are many uncertainties in these kind of calculations. For instance errors in the meteorological data input and the numerical method. To lower the uncertainties when running the HYSPLIT one can generate multiple trajectories from a single meteorological field. (Draxler R. R., 2003).

In this work the air mass trajectories are not directly used. However, any application of this work to real life data would require the use of trajectories. An example of trajectories arriving at a defined point is given in figure 3.

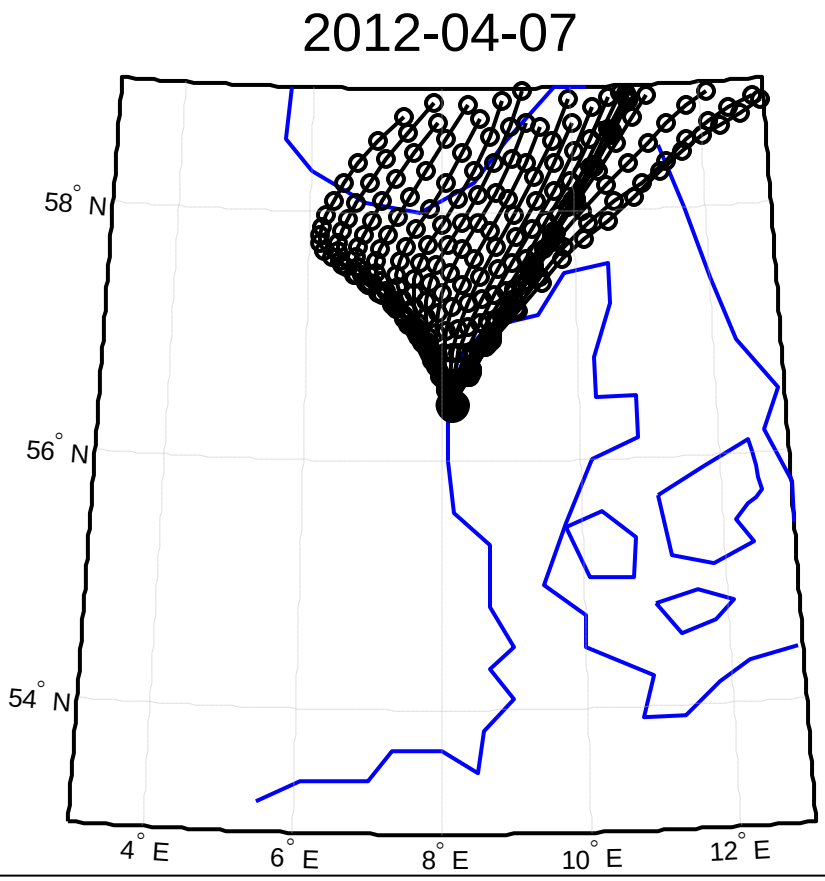

Figure 3: An example of one day of trajectories arriving at a location on the west coast of Denmark. The blue lines are the coast lines, and the black lines are the 24 trajectories arriving at the site (black dot) with one hour intervals. The open circles along the black lines are the positions of the air mass every hour before arriving at the site (one hour resolution).

3. Model

To estimate what effect time- and location dependent particle formation and growth rates have on the observed parameters in a regional NPF events, a new model was created. The model is fundamentally a box model that follows one box of air at the time to a hypothetical measurement station and we see what happens in that box. The different boxes start with different distance from the measurement station, and therefore arrive there at different times with 10 min intervals. The model simulates real measurements by saving only the particle size distribution that arrives at the measurement station and not anything that has happened in the boxes on the way to the station. This resulted in the possibility to observe how new particle formation and growth rates affect the particle size distribution that we measure at the field station.

3.1. Input

The first and one of the most important things to solve was how to input the parameters into the program in a reasonable way. In other words the input needed to be somewhat user friendly where the user does not need to know the program code. The input consists of input for wind speed, growth rate, formation rate and background parameters.

There is a possibility to choose varying time dependent wind speed in the model. However, the wind speed dependence was not examined in the current work, and the wind speed was set to a constant value of 5 m/s throughout all model runs.

Formation and growth rates on the other hand, were either location or time dependent in the different runs. The user starts to choose if the time dependent input should be constant or varying with time using mouse clicks in a plot of formation or growth rate versus time. See the example of time dependent growth rate in figure 4. In the next step, the user chooses if the location dependent input should be constant or varying as function of geographical position. One important thing here is that if the user only wants time or location dependence, the other parameter has to have a constant value of one. The reason for this is due to how the program handles the input of growth and formation rate. The program takes the time dependent value and multiplies it with the location dependent value at a particular time. For example, when the location and time dependent growth rate values are 2 nm/h and 3 nm/h respectively at the same time, the growth rate becomes 6 nm/h. These input choices can be made for both growth and formation rate separately. For instance it is possible to choose only time dependent growth rate and both time and location dependent formation rate.

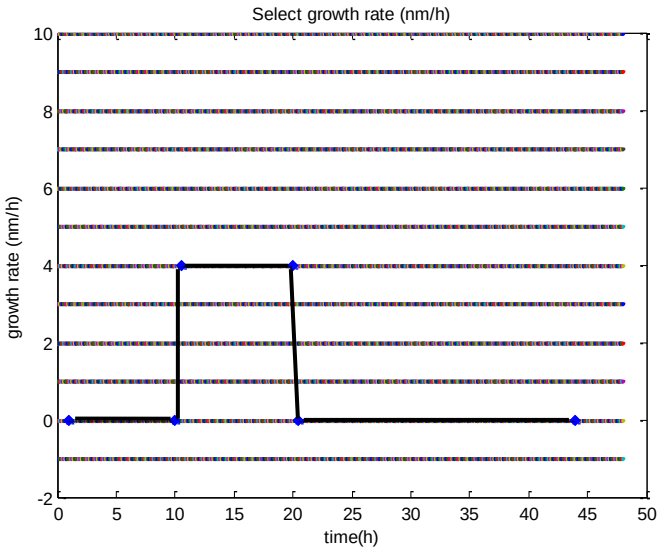

Figure 4: Example of time dependent growth rate chosen by the user. 4 nm/h between 10-20 hours and zero everywhere else.

3.2. The box model

The box model consists of two primary loops. As one can see in figure 5, the arrows illustrate how the boxes move. For instance, the first box starts at the measurement station (location 1) and hence it will just register only one size distribution, since it has already reached the field site. Box number 2 will start at location 2 and after one time step arrive (which was chosen to 10 minutes) at location 1, or in other words at the field site. Box number 3 will go to the location 2 (start location of box number 2) and then to the location 1 which is the measurement station and we register the size distribution in that location. The same will happen for the remaining boxes. Box number 288 will be experiencing 288 time steps, and with a 10 minute resolution this means 48 hours.

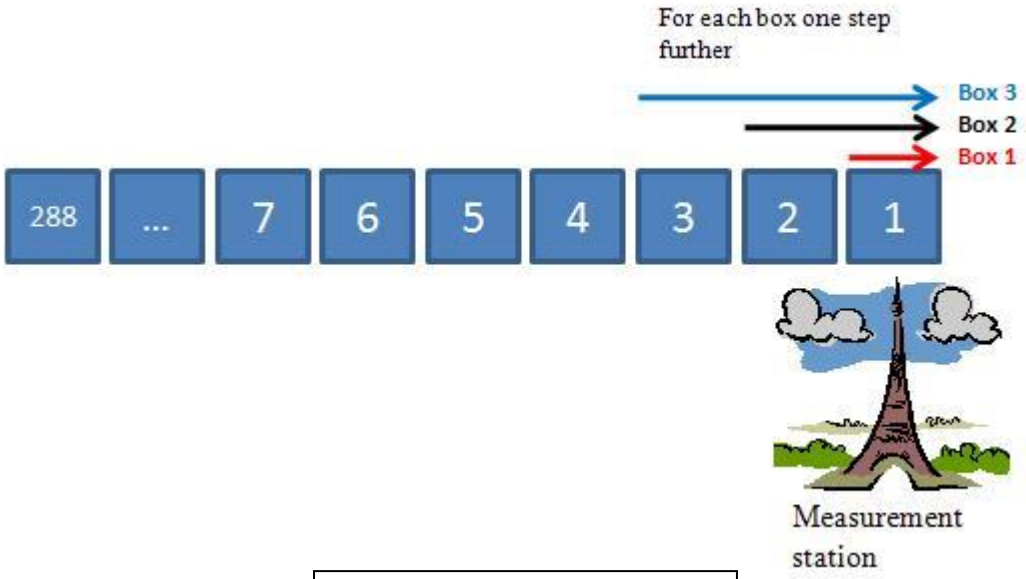

Figure 5: Illustration of how the loops in the box model work.

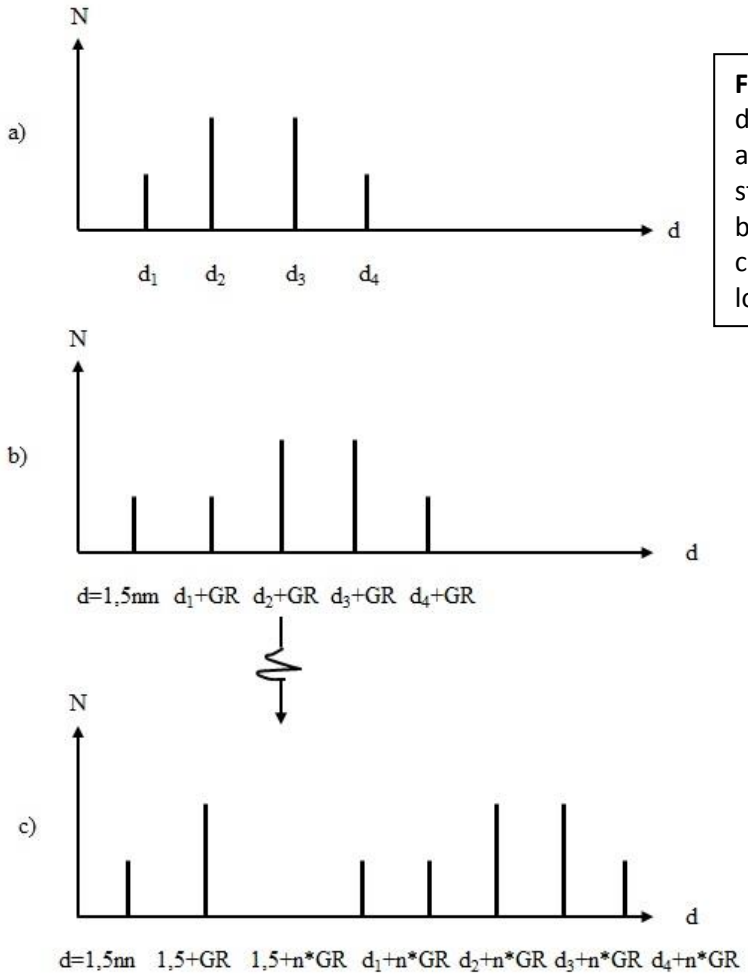

Figure 6: An illustration of the size distribution in one box.
a) Size distribution before first time step.
b) Size distribution after one step.
c) What the size distribution could look like at the measurement station.

The size distribution that every box contains is illustrated in figure 6. Figure 6a shows the background size distribution. This is how the air mass inside the box looks like before the simulation begins. In figure 6b the existing particles grow to larger diameter, at the next time step according to the chosen growth rate during input. If there is an NPF taking place as in the box in figure 6b, the program adds new particles with the size of 1,5 nm into the size distribution. The amount of these particles depends on the formation rate at the time and location of the box. Figure 6c is an illustration of how the size distribution can look like when the box arrives at the measurement station after *n* time steps.

This size distribution illustrated in figure 6 has several discrete particle diameters, since the program uses a linear scale in the simulation. To make the size distribution more comparable to measurements we need to convert it into logarithmic size scale and to use the $dN/d\lg D_p$ size distribution instead of N for the number of particles in different size bins. Normally, size distribution instruments are measuring the particle concentration in discrete size intervals. $dN/d\lg D_p$ is defined as the measured concentration in each size interval divided by the logarithmic width of those intervals. Figure 7 describes an example of how the particles are located in different size bins at the field site when the linear size distribution is converted into a logarithmic one. For the first bin from the left there is only one particle present. In the last size bin there are 6 particles. This binning is used to produce the $dN/d\lg D_p$ distribution (not shown for this oversimplified example).

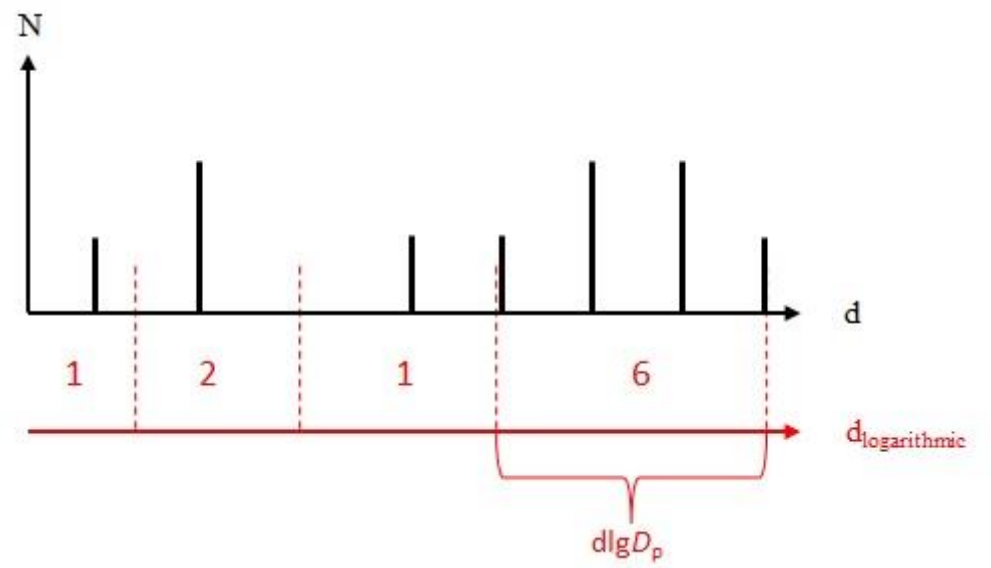

Figure 7: Illustration of how the number concentration as function of discrete particle diameters can be binned into different logarithmic $d\lg D_p$ intervals.

3.3. Aerosol dynamics

The box model contains the aerosol dynamic process of dry deposition, coagulation, and condensation. The dry deposition and coagulation modules are taken from the ADCHEM model (Roldin et al., 2011). Since there are also background particles existing before the onset of new particle formation in the model, these existing particles will also experience condensational growth just like the newly formed particles. To simplify model runs, the condensational growth of the existing particles is set to the same growth rate as the particles from NPF events. Based on other parameterizations of growth rates, this is not an unreasonable assumption (compare with for example Dal Maso et al., 2005).

4. Results

The model is started with a background particle number size distribution containing a particle mode with maximum concentration around the diameter of 80 nm This mode appears in the simulation shown in figure 8 at the simulation time of 0 hours. It appears as a grown mode of particles above 100 nm diameter due to condensation at the station for air masses that arrive later at the hypothetical field station. For simplicity, this background size distribution is always used as input to the model.

4.1. The effects of coagulation and dry deposition

In this first simulation experiment we want to examine how the coagulation and dry deposition look like and how they affect the time dependent number size distribution plot. We performed this by using the exact same parameter setting in all three simulations. The wind speed was constant and set to *5* m/s, growth rate was constant and set to *2* nm/h and the formation rate was $8x10^8$ $m^{-3}h^{-1}$everywhere in the simulation domain, but limited to between 10-15h in the simulation time. (NPF events are more frequent during midday, Kulmala et al., 2004).

In figure 8 the simulation was done with only coagulation. What we expect to see is a decrease in number concentration and an increase in size of the particles in the growing mode of particles formed during the NPF event, which appears as a banana like in Figure 1. In the figure appears as if there might be more particles present in the new particle formation banana at the end of the simulation time. However, this is just an effect of the wider size bins with increasing particle diameter. Hence, although, the color code indicates a higher concentration in the banana at the end of the day, in reality the concentration is lower.

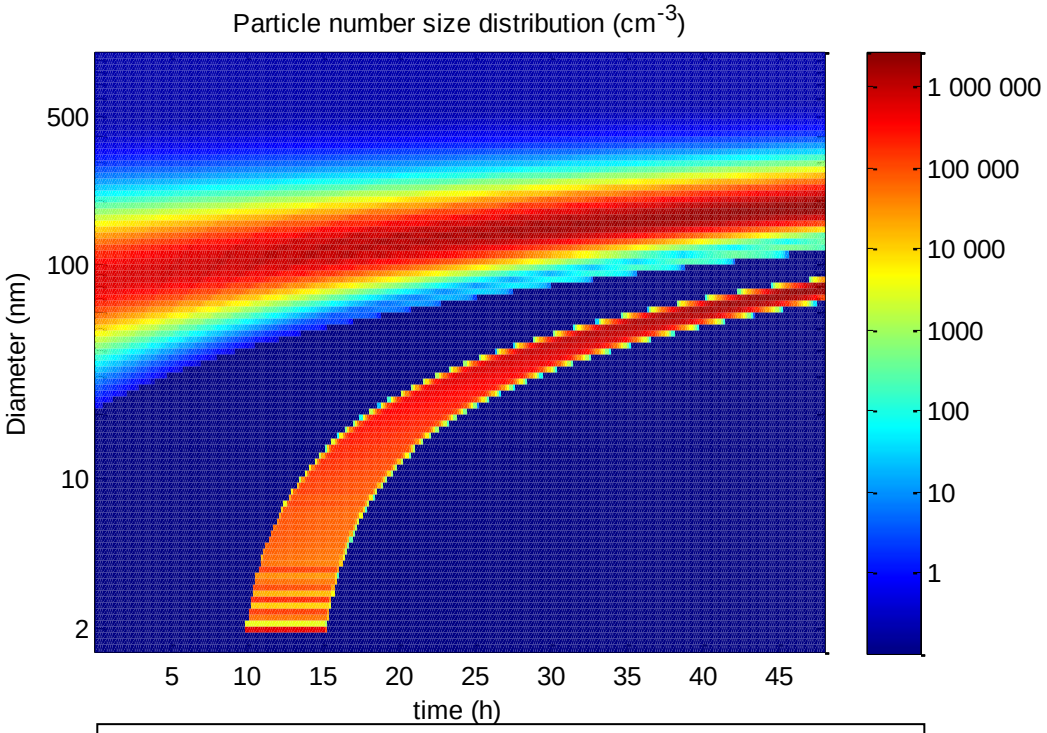

Figure 8: Simulation with only coagulation. Parameters: *WS* = *5*m/s constant, *GR* = *2*mn/h constant and *FR* = $8x10^8$ $m^{-3}h^{-1}$ between 10-15h.

In figure 9 the simulation was done with only dry deposition. The difference in the beginning of the banana compared to figure 8 is that there are more particles in each size bin. Coagulation is most effective for removing the very smallest particles, and since the simulation was done without coagulation we have more particles per size bin in the beginning of the banana where the particles are smallest. The dry deposition continues to be effective for sizes above 10 nm diameter, whereas coagulation stops to be effective for this size range. Hence, the particle concentration continues to decrease also for sizes above 10 nm diameter as can see in figure 9. The relatively more effective removal of particles above 10 nm diameter compared to the coagulation case also depends on that the dry deposition module depends on the time of day. To conclude, coagulation is most effective for the smallest particle sizes, whereas dry deposition is also effective for slightly larger sizes.

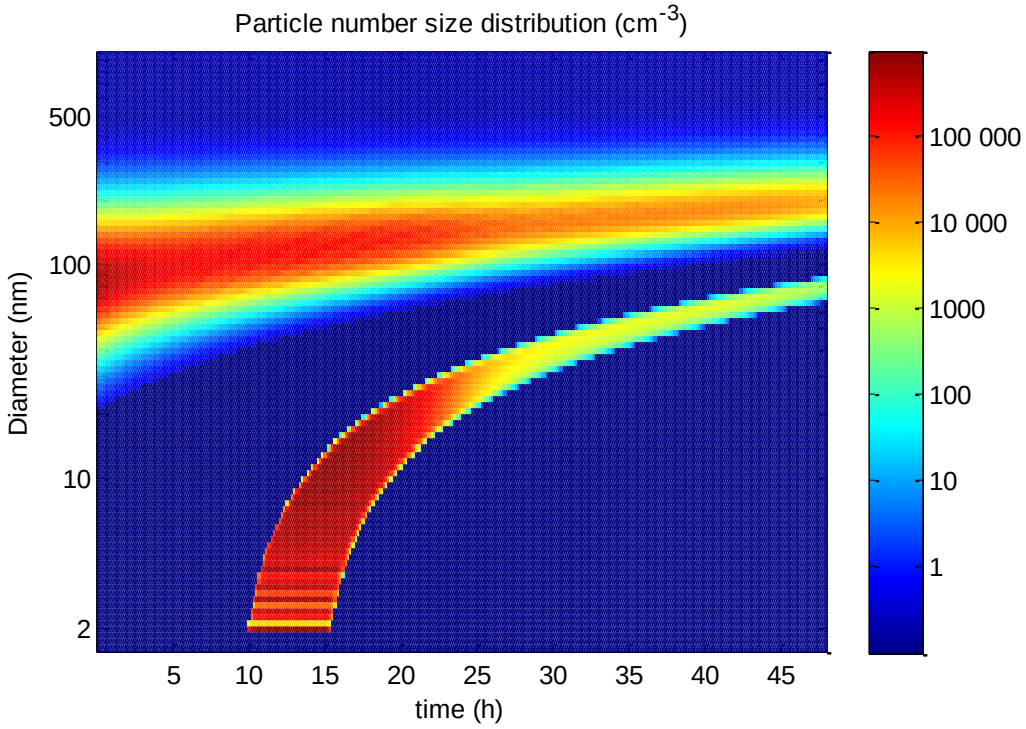

Figure 9: Simulation with only dry deposition. Parameters: *WS* = *5*m/s constant, *GR* = *2*mn/h constant and *FR* = $8x10^8$ $m^{-3}h^{-1}$ between 10-15h.

The simulation that resulted in figure 10 was done with both coagulation and dry deposition. In this simulation we can compare with figure 9. We see the difference in the beginning of the banana due to coagulation. There are less particles in each size bin in figure 10 compared to figure 9. The second thing we can derive from the analysis is that due to the contribution of coagulation the number of particles in the end of the banana is lower than in figure 9.

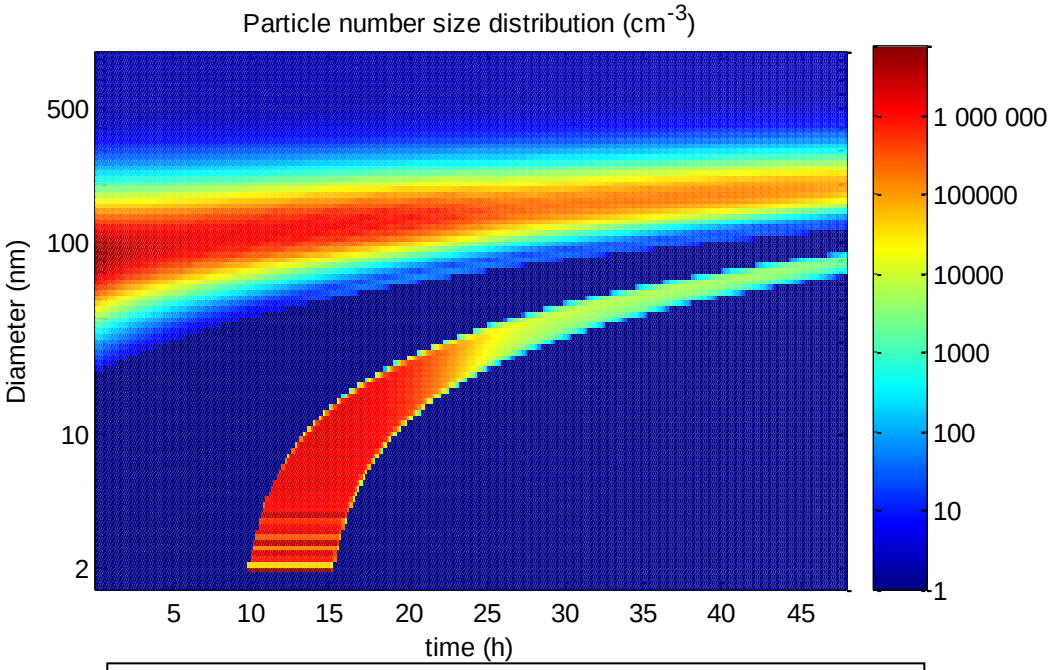

Figure 10: Simulation with both coagulation and dry deposition. Parameters: WS = 5m/s constant, GR = 2mn/h constant and FR = $8x10^{8}$ $m^{-3}h^{-1}$ between 10-15h.

4.2. The effects of time dependent and location dependent particle formation

In this simulation experiment we wanted to see what could be derived from the banana plots for time dependent and location dependent particle formation. Here we used constant wind speed of *5* m/s and constant growth rate of *2* nm/h, we did all simulations without coagulation and dry deposition. The simulation time was 48 hours.

4.2.1. Time dependent particle formation

Here in figure 11 the formation rate was $4x10^{8}$ $m^{-3}h^{-1}$everywhere in the simulation domain, but limited to between 5-10hours of the simulation. In figure 12 the formation rate was $0,13x10^{8}$ $m^{-3}h^{-1}$everywhere in the simulation domain, but limited to between 15-25hours of the simulation. The clear difference we can see between these two is the difference in number concentration of particles in each bin. Figure 11 with higher formation rate has clearly more particles than figure 12. Another finding can be derived from these simulations: If the formation starts earlier in the simulation it will give us bigger particles at the measurement station in the end of the simulation because they have longer time to grow.

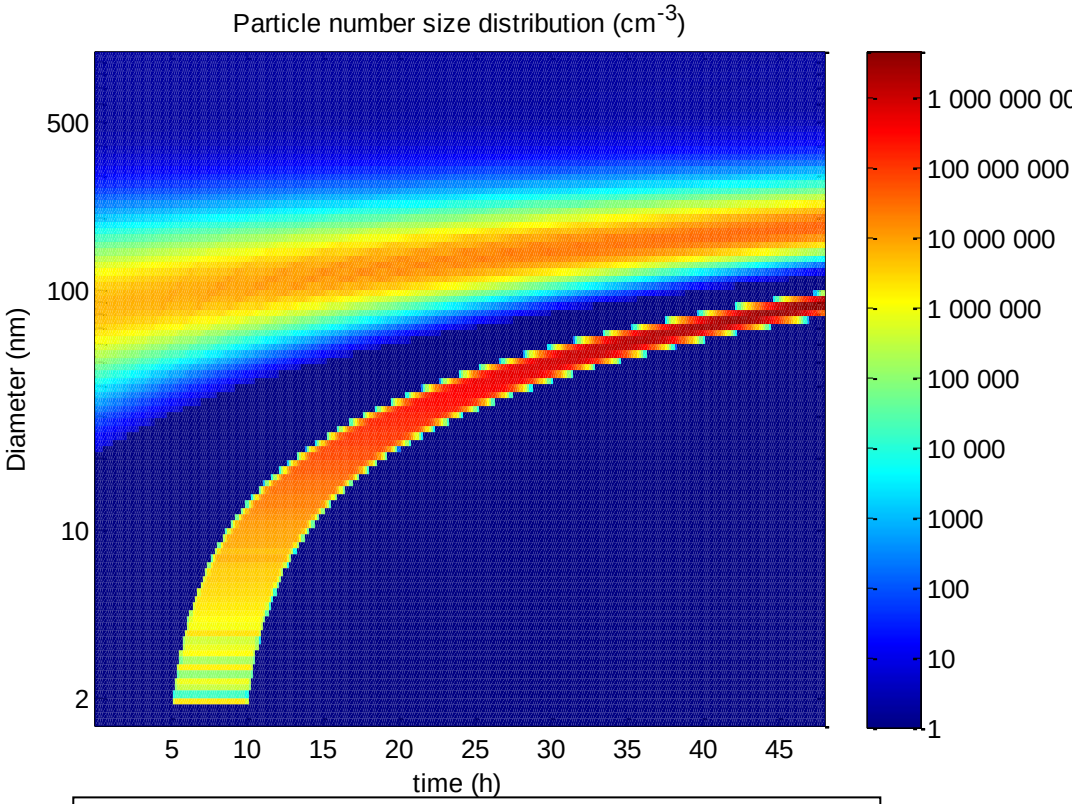

Figure 11: Simulation without coagulation and dry deposition. Parameters: *WS* = *5*m/s constant, *GR* = *2*nm/h constant and *FR(t)* = $4x10^8$ $m^{-3}h^{-1}$ between 5-10h.

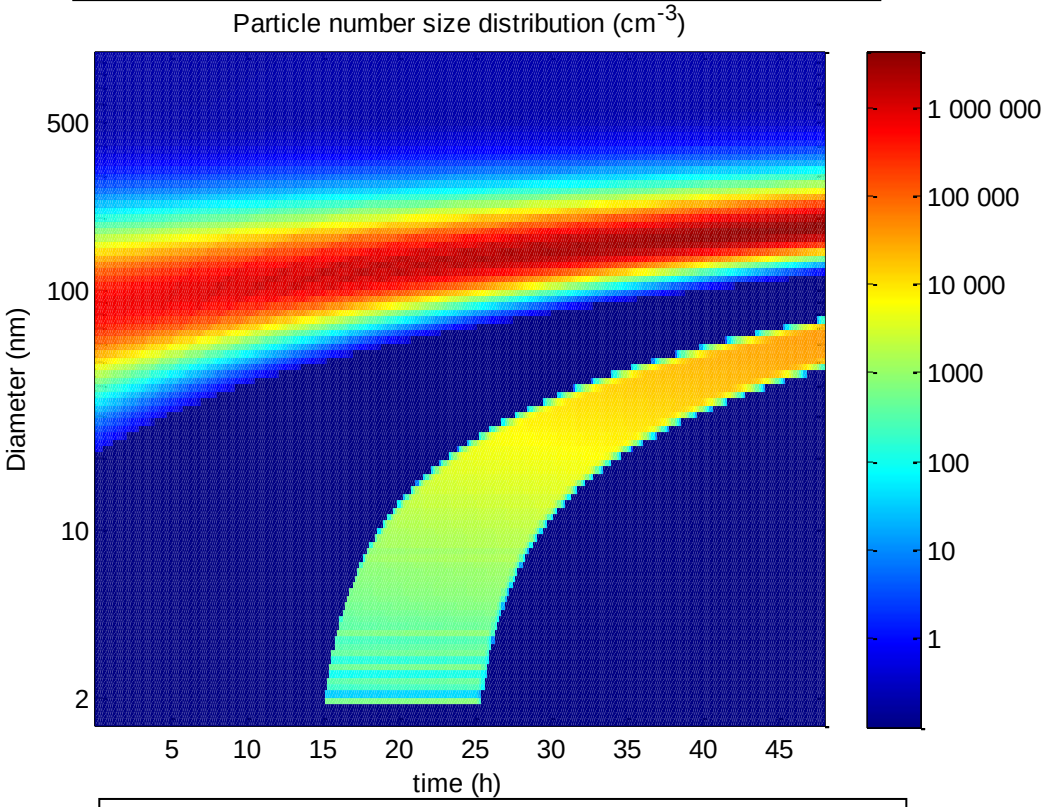

Figure 12: Simulation without coagulation and dry deposition. Parameters: *WS* = *5*m/s constant, *GR* = *2*nm/h constant and *FR(t)* = $0{,}13x10^8$ $m^{-3}h^{-1}$ between 15-25h.

4.2.2. Location dependent particle formation

In figure 13, the formation rate was $8x10^8$ $m^{-3}h^{-1}$at all times between 400 and 600 km from the station and in figure 14 the formation rate was $6x10^8$ $m^{-3}h^{-1}$at all times between 100 and 200 km from the station. The wind speed was *5* m/s, the growth rate was *2* nm/h and there were no coagulation or dry deposition in both runs presented.

The figures show that the particles have different time to grow depending on where the formation took place. Besides, when the formation rate is only location dependent, the particles can form only in a limited area, meaning that all particles that arrive at the measurement station have roughly the same size ("knife" in Figures 13 and 14 instead of the classical banana-shaped distribution). The small slope in the beginning of the "knife" in both figure 13 and 14 is due to some boxes starting their path in the end of the formation area so they had a slightly shorter time to grow compared to the boxes that start further away or beyond the formation area. As can be seen in figure 13, all particles are around 80 nm at the station in the "knife" distribution, while they are around 20 nm diameter in figure 14. The particles in the first simulation have been formed further away from the station.

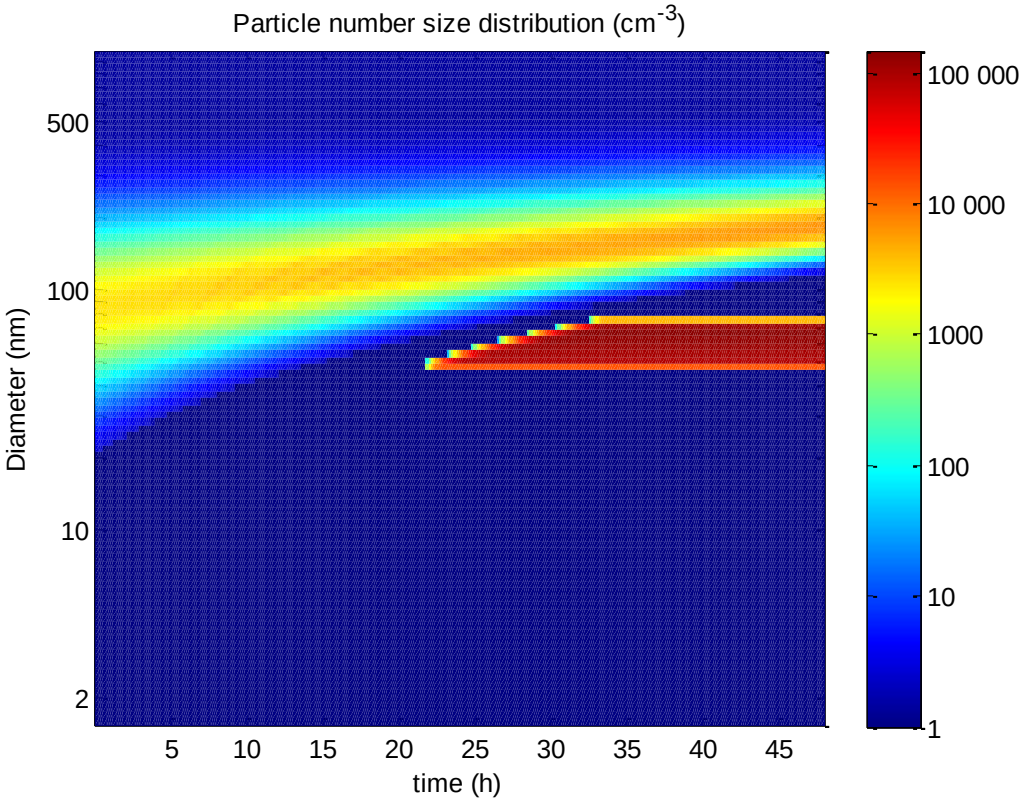

Figure 13: Simulation without coagulation and dry deposition. Parameters: *WS* = *5*m/s constant, *GR* = *2*nm/h constant and *FR(x)* = $8x10^8$ $m^{-3}h^{-1}$ between 400 and 600 km from the station.

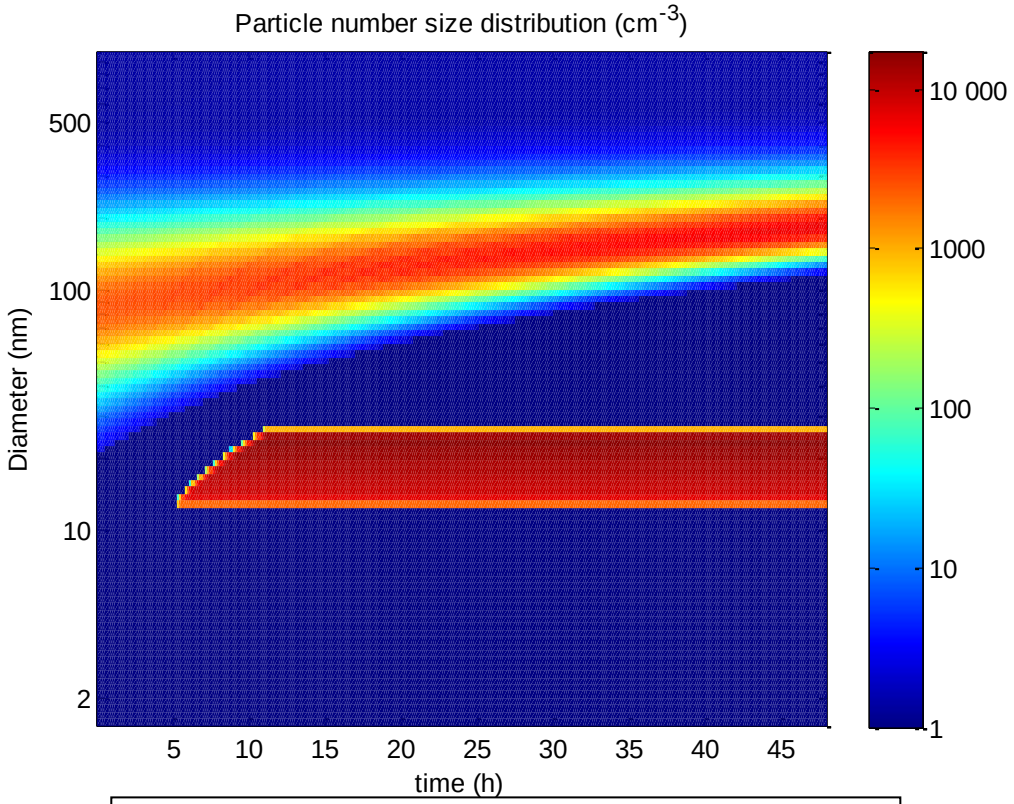

Figure 14: Simulation without coagulation and dry deposition. Parameters: *WS* = *5*m/s constant, *GR* = *2*nm/h constant and *FR(x)* = $6x10^8$ $m^{-3}h^{-1}$ between 100 and 200 km from the station.

4.2.3. Time and location dependent particle formation

We now tested to use both a time and location dependent formation in the next run, shown in Figure 15. The parameters were: wind speed constant at *5* m/s, growth rate constant at *2* nm/h and no coagulation or dry deposition. The formation rate is: *FR(t)* = $8x10^8$ $m^{-3}h^{-1}$ between 10-15 hours. *FR(x)* = $8x10^8$ $m^{-3}h^{-1}$ between 300 and 500 km from the station.

In this simulation the particles could form only at a specific place at a specific time. So the air mass that was located at 300 km from the station at the start of the formation window (10 hours) contains the smallest particles that arrive at the measurement station at the time of 25 hours. The air mass that was located at 500 km from the station at the end of the formation window contains the particles that were formed furthest away from the station and hence are also larger due to longest growth time. Everywhere else there is no formation of particles. The horizontal extent of the "banana" for each size bin is dictated by the width of the formation time window and the vertical extent of the "banana" is defined by the width of the formation area and the growth rate. In reality this type of event could happen when a limited forest area will form particles when there is sunlight and the formation ends when the sun sets.

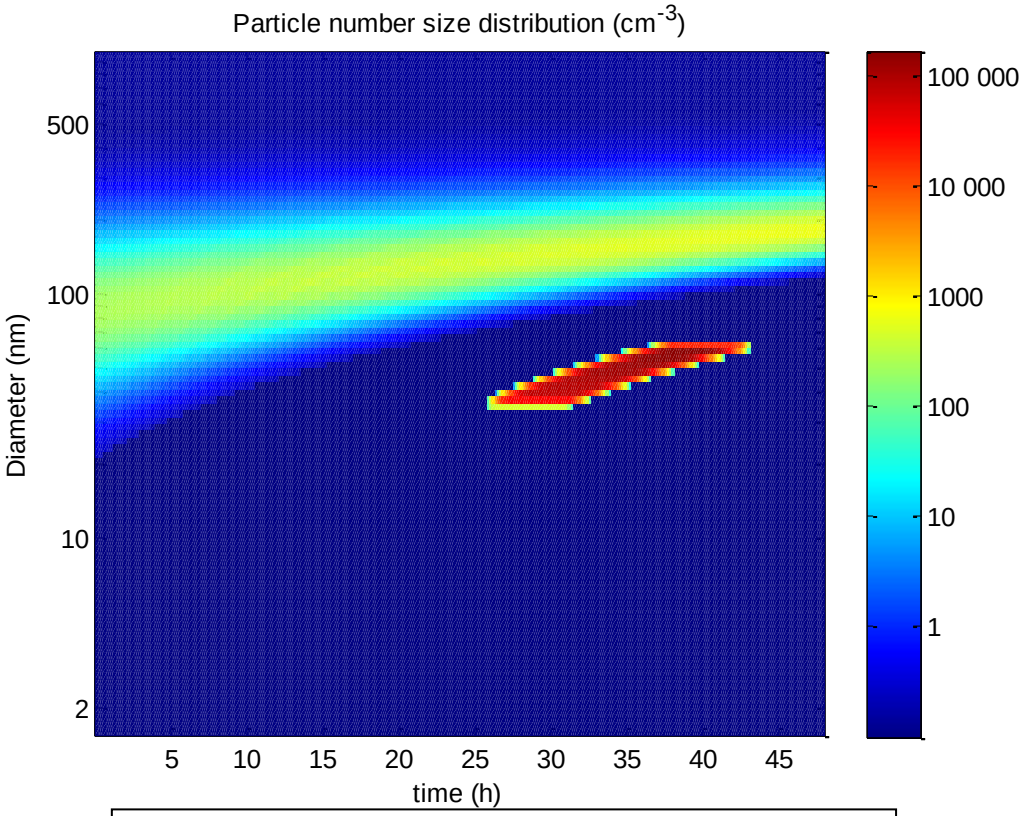

Figure 15: Simulation without coagulation and dry deposition. Parameters: *WS* = *5*m/s constant, *GR* = *2*nm/h constant and *FR(t)* = $8x10^8$ $m^{-3}h^{-1}$ between 10-15h, *FR(x)* = $8x10^8$ $m^{-3}h^{-1}$ between 300 and 500 km from the station.

4.3. The effects of time dependent and location dependent particle growth

All simulations on the effects of growth rate were done without coagulation and dry deposition. The wind speed was *5* m/s and the formation rate was $8x10^8$ $m^{-3}h^{-1}$everywhere in the simulation domain, but limited to between 10-15 hours in the simulation time of 48 hours. What we expect to observe in the experiments with only time dependence is a constant size of all particles outside the growth rate time that we assigned. What we expect to observe in the experiments with only location dependent growth is that all particles will grow the same amount, almost like in the location dependent experiments with the formation rate (chapter 4.2.2), only that the particles will have a growth banana from formation size to the size they reach depending on how much time they have spent in the growth area.

4.3.1. Time dependent particle growth

In figure 16 the growth rate was *6* nm/h everywhere in the simulation domain, but limited to between 10-15 hours. The formation rate was $8x10^8$ $m^{-3}h^{-1}$ everywhere, but limited to between 10-15 hours, wind speed was *5* m/s. Figure 17 had all the same parameters as figure 16 except that the growth rate was *4* nm/h everywhere, but limited to between 25-45 hours of the simulation time. So both figure 16 and 17 are very similar in parameter set-up, but look very different from one another. The reason for this is the growth and formation happened at the same time in figure 16, but not in figure 17. That's why there are particles for every size, from

the particles that had longest time to grow at the maximum size to the smallest size of particles that can be seen with this simulation. In figure 17 the growth happened after the particles were formed. The reason why the banana is so narrow is because when the growth started, all particles had the same size and all particles continue to have the same sizes during growth. If this simulation would have been performed with coagulation and dry deposition included, the particles would have been taken out before the growth started.

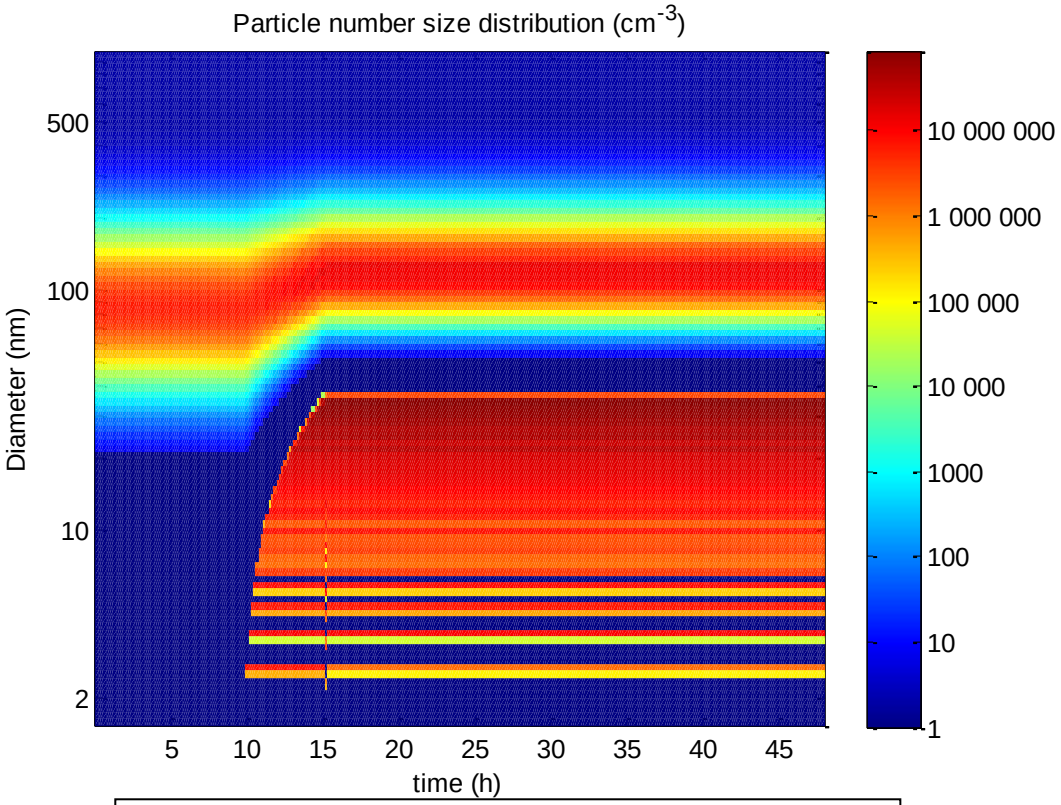

Figure 16: Simulation without coagulation and dry deposition. Parameters: *WS = 5* m/s, $FR(t) = 8x10^{8}$ $m^{-3}h^{-1}$ between 10-15h, *GR(t) = 6* nm/h between 10-15 h.

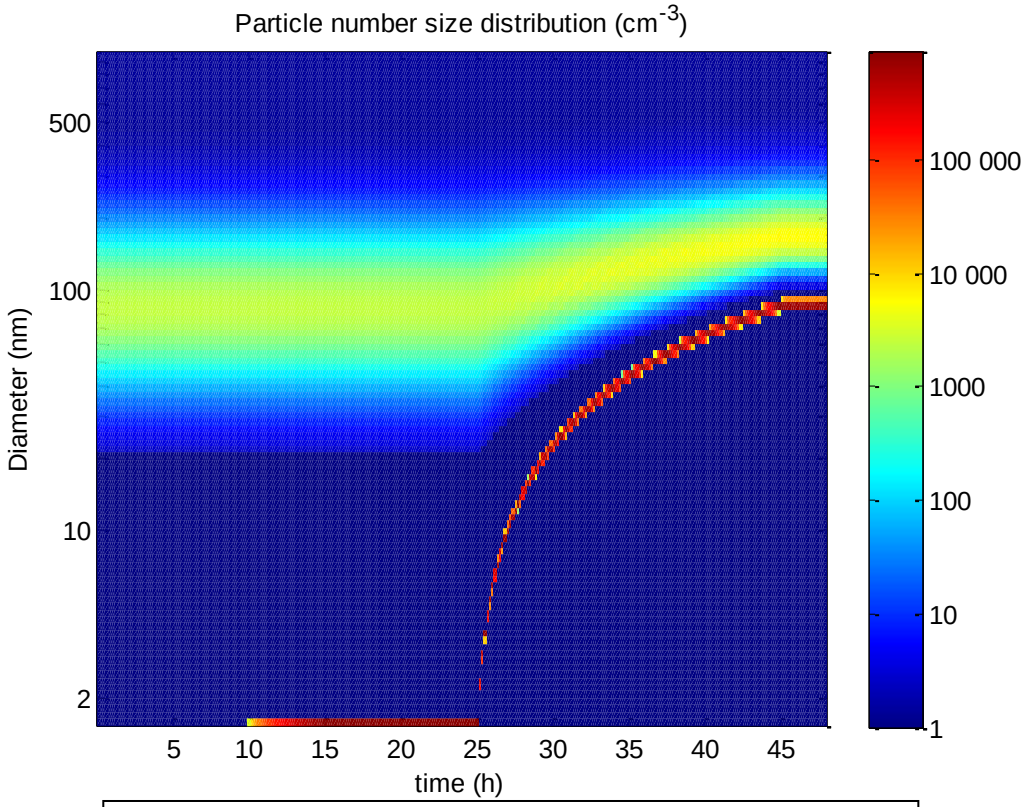

Figure 17: Simulation without coagulation and dry deposition. Parameters: *WS = 5* m/s, *FR(t) = 8x10*^{8} m^{-3}h^{-1} between 10-15h, *GR(t) = 4* nm/h between 25-45 h.

4.3.2. Location dependent particle growth

In figure 18 the growth rate was *3* nm/h at all times between 300 and 500 km from the measurement station, formation rate was *8x10*^{8} m^{-3}h^{-1} everywhere, but limited to between 10-15 hours, and wind speed was *5* m/s. The growth cannot be observed until after 26 hours. The particles formed 300 km from the station reached the station 26 hours later. The particles formed 500 km from the station reached the station 42 hours later. All particles that have their formation further away from the station then 500 km will all have approximately the same size since they spend the same amount of time in the growth area. These particles represent the population of particles at the end of the banana when the curve becomes horizontal. The background particles appear to start to grow earlier than the NPF particles in the size distribution observed at the station, since they were introduced in the box model 10 hours earlier. Hence they will arrive at the growth area 10 hours earlier.

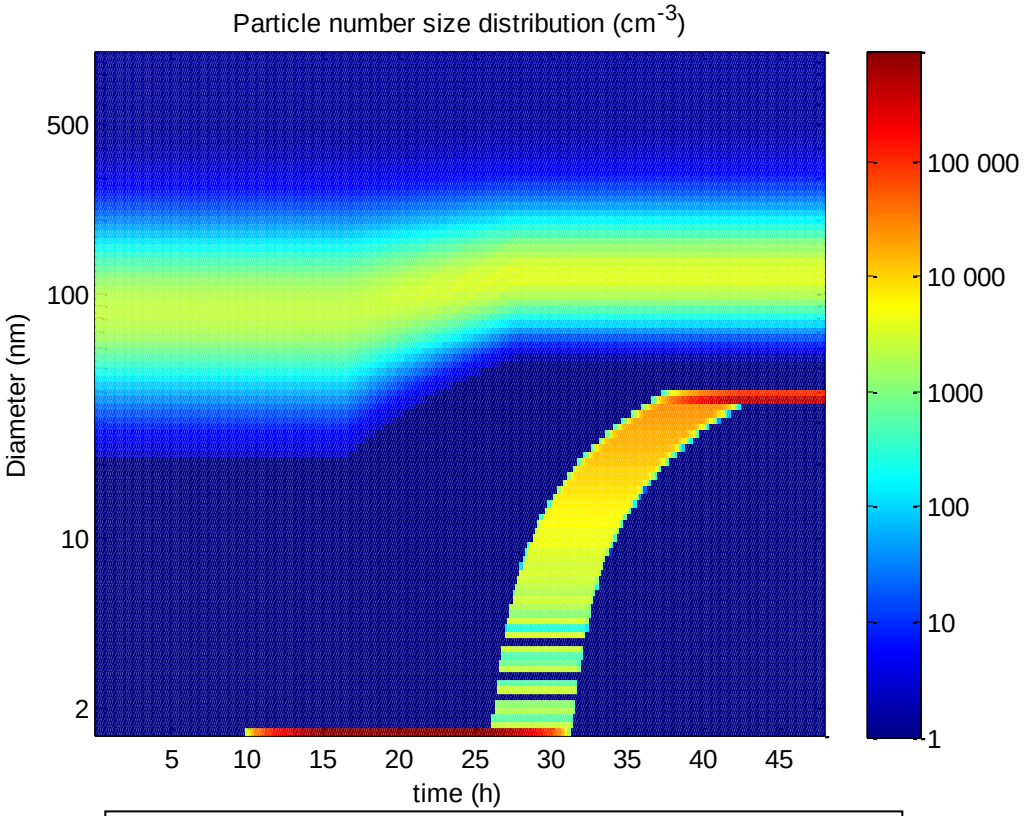

Figure 18: Simulation without coagulation and dry deposition. Parameters: *WS = 5* m/s, *FR(t) = 8x10*^{8} m^{-3}h^{-1} between 10-15h, *GR(x) = 3* nm/h between 300 and 500 km from the station.

4.3.3. Time and location dependent particle growth

Both time and location dependent particle growth was simulated in the box model, and the results can be seen in figure 19. This simulation was done without coagulation and dry deposition. The parameters used in figure 19 were growth rate *GR(t) = 2* nm/h between 15-20 hours, *GR(x) = 3* nm/h between 200 and 300 km from the station, formation rate was *8x10*^{8} m^{-3}h^{-1} everywhere, but limited to between 10-15 hours, wind speed 5 m/s.

The growth rate attributed to a limited time and area window produced the "shark"-like shape of the size distribution of the NPF particles. All particles are formed before the growth rate time window and are the reason for the narrow banana shape. When the time dependent growth starts, the particles 300 km from the station will have most time to grow, and will grow to the biggest sizes while the particles half way through the location dependent growth area will be the particles in the first part of the shark looking banana. The second part consists of the particles halfway through the location dependent growth area at the time that the time dependent formation window closes. This flow through the time and location dependent area is schematically explained in figure 20.

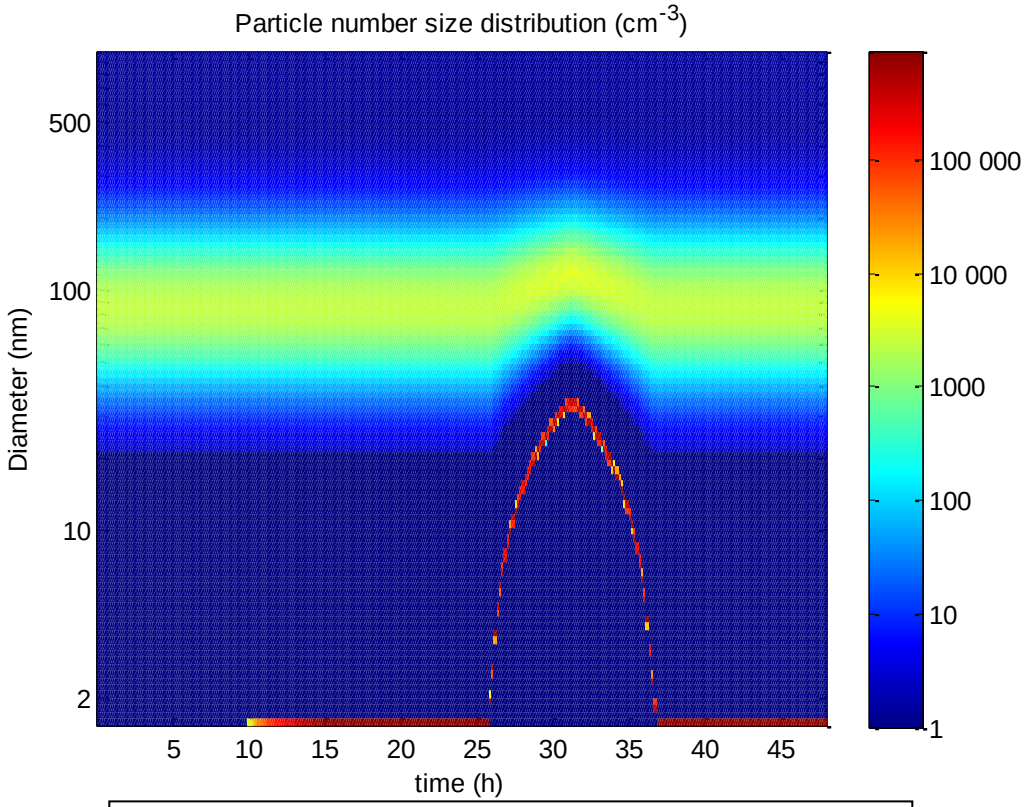

Figure 19: Simulation without coagulation and dry deposition. Parameters: *WS = 5* m/s, *FR(t) = 8x10*^{8} m^{-3}h^{-1} between 10-15h, *GR(t) = 2* nm/h between 15-20h, GR(x) = 3 nm/h between 300-200 km from the station.

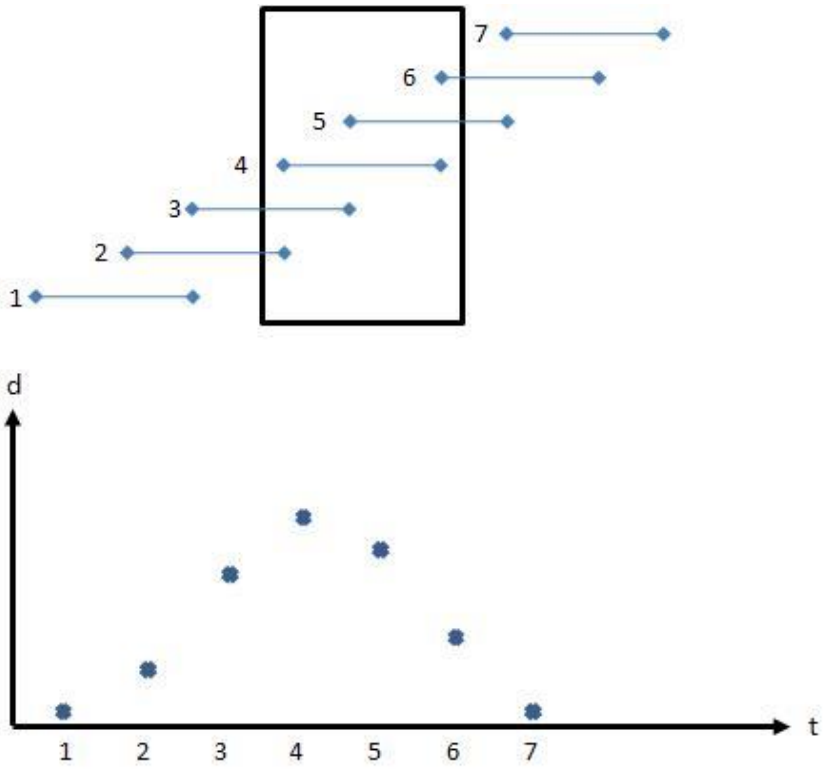

Figure 20: An illustration of how the time and location dependent growth works. The square is the location dependent growth window and the numbered lines in it are depicting where the particles are located during the growth time. The graph at the bottom shows the final size the particles as a function of time spent in the growth area during the growth time window.

5. Conclusions and discussion

The analysis shows how the time and location dependent formation is influencing the size distribution at the hypothetical field site. For time dependent NPF, the banana-shaped NPF event growth from the smallest of particles and consists of a full banana up to the maximum size achieved for the longest growth duration. The width of the banana depends on the length of the formation time window.

The location dependent NPF resulted in a banana knife shaped size distribution at the field station. All particles were of approximately the same size. The absolute size of the particles depends on where the NPF happened, and thus how long time the particles had to grow. The vertical width of the banana depends on how large the formation area was.

The time and location dependent NPF resulted in the size distribution in figure 15. By analyzing figure 15 it is possible to calculate when the NPF event took place and also how large the formation area was.

The location and time dependent growth rate can also be studied, for example as in the simulation corresponding to figure 16. The figure unfortunately also gaps where it appears that there are no particles at all. These gaps are created when the program is converting the linear particle number size distribution into a logarithmic distribution. Some bins size limits are defined between two sequential particle sizes and that is why these become empty of particles.

Due to the location dependent particle growth, it seems that the background particles and NPF particles are not growing at the same time. This is actually true. Namely, the background particles are formed earlier in the model run.

When we used both time and location dependent growth we got a shark-like structure of the NPF event particles as a result. This was a valid result and could possibly be happening in real life. One example is a situation when there is an island in the ocean and the growth could only occur when the air was over the island during certain hours of the day.

Most simulations were done without coagulation and dry deposition. These processes would have affected many of the simulations in a major way, especially in the simulations where the NPF occurred before the growth. In a model run with both process introduced, all nanometer sized particles formed during the NPF event would have been removed through coagulation or dry deposition before the growth started. Hence, the smallest particles would not remain before the growth started.

In real life, it is likely that the NPF particles would not remain in the atmosphere either. This is the only unrealistic simulation in the present study. All other cases could be regarded as likely to happen in the atmosphere, although the absolute values and timing of the NPF events need not to be exactly the same in atmosphere.

This work is one piece of the puzzle needed to understand the observations of NPF events at actual field stations. Future research should include quantifying the effects of varying NPF parameters better and applying the box model to real life NPF analysis. To improve the model further, changing wind speed and mixing conditions should be handled and tested in different model runs. It would be important to investigate if regular NPF banana observed at the

measurement stations, like in figure 1 could be reproduced in the model by changing wind speed conditions and by selecting different values of the formation and growth rate.

6. Acknowledgements

This bachelor thesis was done at the Division of Nuclear Physics at the Department of Physics at Lund University. I would like to thank my supervisors Niku Kivekäs and Adam Kristensson for their help and guidance during the work of this thesis. I am also thankful for their flexibility on the time table of the thesis so I was able to perform it during the summer. Finally I would like to thank Pontus Roldin for his contributions to the simulation model.

7. References

Asmi, E., Sipilä, M., Manninen, H. E., Vanhanen, J., Lehtipalo, K., Gagné, S., Neitola, K., Mirme, A., Mirme, S., Tamm, E., Uin, J., Komsaare, K., Attoui, M., and Kulmala, M. (2009): Results of the first air ion spectrometer calibration and intercomparison workshop, Atmos. Chem. Phys., 9, 141-154, doi:10.5194/acp-9-141-2009.

Dal Maso, M., Kulmala, M.,Riipinen, I., Wagner, R., Hussein, T., Aalto, P. P., and Lehtinen, K. E. J. (2005).Formation and growth of fresh atmospheric aerosols: eight years of aerosol size distribution data from SMEAR II, Hyytiälä, Finland. Boreal Environ. Res., 10, 323-336.

Draxler, R.R., and G.D. Hess, (1998): An overview of the HYSPLIT_4 modeling system of trajectories, dispersion, and deposition. Aust. Meteor. Mag., 47, 295-308.

Draxler, R.R. (2003), Evaluation of an ensemble dispersion calculation, Journal of Applied Meteorology, Vol. 42, February, 308-317.

Frank, G.(2001). Experimental studies of the interaction of atmospheric aerosol particles with clouds and fogs, ISBN 91-7874-169-6, Doctoral dissertation at Lund University, Dep. of Nuclear physics, Lund, Sweden.

Hinds, W. C. (1998). Aerosol Technology, New Your, USA, John Wiley & Sons, Inc., 2. edition.

Hinds, W, C. (1999). Aerosol technology: properties, behavior, and measurement of airborne particles.

Hussein, T., Junninen, H., Tunved, P., Kristensson, A., Dal Maso, M., Riipinen, I., Aalto, P. P., Hansson, H.-C., Swietlicki, E., and Kulmala, M. (2009): Time span and spatial scale of regional new particle formation events over Finland and Southern Sweden, Atmos. Chem. Phys., 9, 4699-4716, doi:10.5194/acp-9-4699-2009.

IPCC, (2012): Managing the Risks of Extreme Events and Disasters to Advance ClimateChange Adaptation. A Special Report of Working Groups I and II of theIntergovernmental Panel on Climate Change [Field, C.B., V. Barros, T.F. Stocker,D. Qin, D.J. Dokken, K.L. Ebi, M.D. Mastrandrea, K.J. Mach, G.-K. Plattner, S.K. Allen,M. Tignor, and P.M. Midgley (eds.)]. Cambridge University Press, Cambridge, UK,and New York, NY, USA, 582 pp.

Kerminen, V.-M., Lehtinen, K., Anttila, T. and Kulmala, M. (2004). Dynamics of atmospheric nucleation mode particles: a timescale analysis, *Tellus B*, 56 (2), 135-146.

Kerminen, V.-M., H. Lihavainen, M. Komppula, Y. Viisanen, and M. Kulmala (2005), Direct observational evidence linking atmospheric aerosol formation and cloud droplet activation, Geophys. Res. Lett., **32**, L14803, doi:10.1029/2005GL023130.

Komppula, M., Sihto, S.L., Korhonen, H., Lihavainen, H., Kerminen, V.M., Kulmala, M. &Viisanen, Y. (2006), "New particle formation in air mass transported between two measurement sites in Northern Finland", Atmospheric Chemistry and Physics, vol. 6, no. 10, pp. 2811-2824.

Kristensson, A. (2012). A compendium in atmospheric aerosol particles for the atmospheric chemistry course, Lund University, Department of Physics, Division of Nuclear Physics.

Kulmala, M., Vehkamaki, H., Petaja, T., Dal Maso, M., Lauri, A., Kerminen, V.-M., Birmili, W., and McMurry, P. (2004): Formation and growth rates of ultrafine atmospheric particles: a review of ob- servations, J. Aerosol Sci., 35, 143–176.

Kulmala, M.,Kontkanen, J.,Junninen,H.,Lehtipalo, K.,Manninen, H. E.,Nieminen, T.,Petäjä, T.,Sipilä, M.,Schobesberger, S.,Rantala, P.,Franchin, A.,Jokinen, T., Järvinen, E.,Äijälä, M.,Kangasluoma, J.,Hakala, J., Aalto, P. P., Paasonen,P.Mikkilä, J.,Vanhanen, J., Aalto, J.,Hakola, H., Makkonen, U.,Ruuskanen, T., Mauldin III, R. L.,Duplissy, J., Vehkamäki, H.,Bäck, J.,Kortelainen, A.,Riipinen, I.,Kurtén, T., Johnston, M. V., Smith, J. N.,Ehn, M.,Mentel, T. F., Lehtinen, K. E. J.,Laaksonen, A.,Kerminen, V-M.,Worsnop, D. R., (2013). Direct Observations ofAtmosphericAerosol Nucleation.

Krejci, R., Ström, J., de Reus, M., Williams, J., Fischer, H., Andreae, M. O., and Hansson, H.-C. (2005): Spatial and temporal distribution of atmospheric aerosols in the lowermost troposphere over the Amazonian tropical rainforest, Atmos. Chem. Phys., 5, 1527-1543, doi:10.5194/acp-5-1527-2005.

Kyrö, E.-M., Kerminen, V.-M., Virkkula, A., Dal Maso, M., Parshintsev, J., Ruíz-Jimenez, J., Forsström, L., Manninen, H. E., Riekkola, M.-L., Heinonen, P., and Kulmala, M. (2012): Antarctic new particle formation from continental biogenic precursors, Atmos. Chem. Phys. Discuss., 12, 32741-32794, doi:10.5194/acpd-12-32741-2012.

Manninen, H. E., Petäjä, T., Asmi, E., Riipinen, I., Nieminen, T., Mikkilä, J., Hõrrak, U., Mirme, A., Mirme, S., Laakso, L., Kerminen, V.-M. Kulmala, M. (2009): Long-term field measurements of charged and neutral clusters using Neutral cluster and Air Ion Spectrometer (NAIS). Boreal Env. Res. 14: 591–605.

Merikanto J., Spracklen D. V., Mann G. W., Pickering S. J., and Carslaw K. S., (2009). Impact of nucleation on global CCN.

Roldin, P., Swietlicki, E., Schurgers, G., Arneth, A., Lehtinen, K. E. J., Boy, M., and Kulmala, M. (2011). Development and evaluation of the aerosol dynamics and gas phase chemistry model ADCHEM. Atmos. Chem. Phys., 11, 5867-5896.

Seinfeld, J. H., Pandis, S. N., (2006). Atmospheric chemistry and physics: From air pollution to climate change – 2nd edition.

Slinn, W. et al. (1982), Predictions for particle deposition to vegetative canopies, Atmospheric Environment, vol. 16.

Väänänen, R., Kyrö, E.-M., Nieminen, T., Kivekäs, N., Junninen, H., Virkkula, A., Dal Maso, M., Lihavainen, H., Viisanen, Y., Svenningsson, B., Holst, T., Arneth, A., Aalto, P. P., Kulmala, M., and Kerminen, V.-M. (2013): Analysis of particle size distribution changes between three measurement sites in Northern Scandinavia, Atmos. Chem. Phys. Discuss., 13, 9401-9442.

8. Appendix

8.1 Simulation Model code

```
clearall;

simulation_time=48;              % simulations time in hours
time_steps=6*simulation_time;    % number of time steps
WS=zeros(time_steps:1);          % Wind speed vector
GR=zeros(time_steps:1);          % Growth rate vector
Jnucl=zeros(time_steps:1);       % Formation rate vector

%%%%%%%%%% Input grafically the wind speed for the simulation time %%%%%%%%
%interrupt1=menu('Press','Select wind speed(m/s)','Constant wind speed');
%    if interrupt1==2
%        interrupt1=true;
%    else
%        interrupt1=false;
%    end
%
%    if interrupt1
%%%%%%%%%%%%%%%% Input window for wind speed%%%%%%%%%%%%%%%%%%%%%%%%%%%%%%%
        prompt = {'Enter constant wind speed(m/s):'};
dlg_title = 'Input';
num_lines = 1;
def = {'1'};
answerWS = inputdlg(prompt,dlg_title,num_lines,def);

%%%%%%%%%%Conversion from cell to double%%%%%%%%%%%%%%%%%%%%%%%%%%%%%%%%%%
E = sprintf('%s*', answerWS{:});
inputWS = sscanf(E, '%f*');   %Input values in double instead of cell
%%%%%%%%%%%%%%%%%%%%%%%%%%%%%%%%%%%%%%%%%%%%%%%%%%%%%%%%%%%%%%%%%%%%%%%%%%%
%%%%%%%

%%%%%%%%%%%%%%%%%%%%%%%%%%%%%%%%%%%%%%%%%%%%%%%%%%%%%%%%%%%%%%%%%%%%%%%%%%%
%%%%%%%
%     else
%
a=0.1;b=4;c=6;d=8;e=10;f=12;g=14;h=16;i=18;j=20;k=22;l=24;m=2;n=-1;y=0:0.1:48;
%
%         figure(1);clf;
%         plot(y,a,'-',y,b,'-',y,c,'-',y,d,'-',y,e,'-',y,f,'-',y,g,'-',y,h,'-',y,i,'-',y,j,'-',y,k,'-',y,l,'-',y,m,'-',y,n,'-');
%         xaxis=[0 1 2 3 4 5 6 7 8 9 10 11 12 13 14 15 16 17 18 19 20 21 22 23 24 25 26 ...
%             27 28 29 30 31 32 33 34 35 36 37 38 39 40 41 42 43 44 45 46 47 48];
%         yaxis=[0 1 2 3 4 5 6 7 8 9 10 11 12 13 14 15 16 17 18 19 20 21 22 23 24 25];
%         title('Select wind speed(m/s)');
```

```
%         xlabel('time(h)');
%         ylabel('Wind speed(m/s)');
%
%         [intime,inWS]=ginput();
%         for p=1:length(inWS)
%             ifinWS(p,1)<0
%                 inWS(p,1)=1;
%             end;
%         end;
%         intime(1,1)=0.2;
%         intime(length(intime),1)=48;
%         sumWS=zeros(288:1);
%         sumWS(1,1)=inWS(1,1);
%
%         for x=2:length(intime);
%             timesteps(x-1)=floor((intime(x,1)*6))-floor((intime(x-1,1)*6));
%
%             startt(x-1)=floor(intime(x-1,1)*6);
%             dWS=inWS(x,1)-inWS(x-1,1);
%             dWSt=dWS/timesteps(x-1);
%
%             for z=1:timesteps(x-1)
%                 sumWS(startt(x-1)+z,1)=sumWS(startt(x-1)+z-1,1)+dWSt;
%                 if sumWS(startt(x-1)+z,1)<0
%                     sumWS(startt(x-1)+z,1)=0;
%                 end;
%             end;
%         end;
%     end;
%%%%%%%%%%%%%%%%%%%%%%%%%%%%%%%%%%%%%%%%%%%%%%%%%%%%%%%%%%%%%%%%%%%%%%%%%%%%%%

%if interrupt1
for q=1:time_steps
    WS(q,1)=inputWS;     %Constant wind speed
end;
%else
%    WS=sumWS;             %wind speed
%end;

Location(1:time_steps)=0;        %The location of the measurement station
for t=time_steps:-1:2
    Location(t-1)=Location(t)-WS(t,1)*600;    %The location of the box
end;

%%%%%%%%%% Input grafically the growth rate for the simulation time %%%%%%%
interrupt2=menu('Press','Select growth rate over time(nm/h)','Constant growth rate over time');
if interrupt2==2
```

```
        interrupt2=true;
else
        interrupt2=false;
end

if interrupt2
%%%%%%%%%%%%%%% Input window for growth rate%%%%%%%%%%%%%%%%%%%%%%%%%%%%%%%
        prompt = {'Enter constant growth rate(nm/h):'};
dlg_title = 'Input';
num_lines = 1;
def = {'2'};
answerGR = inputdlg(prompt,dlg_title,num_lines,def);

%%%%%%%%%%%Conversion from cell to double%%%%%%%%%%%%%%%%%%%%%%%%%%%%%%%%%%
R = sprintf('%s*', answerGR{:});
inputGR = sscanf(R, '%f*');   %Input values in double instead of cell
%%%%%%%%%%%%%%%%%%%%%%%%%%%%%%%%%%%%%%%%%%%%%%%%%%%%%%%%%%%%%%%%%%%%%%%%%%%%%%%%%%%
else
        a=1;b=2;c=3;d=4;e=5;f=6;g=7;h=8;i=9;j=10;k=0;n=-1;y=0:0.1:48;

figure(2);clf;

        plot(y,a,'-',y,b,'-',y,c,'-',y,d,'-',y,e,'-',y,f,'-',y,g,'-',y,h,'-',y,i,'-',y,j,'-',y,k,'-',y,n,'-');
xaxis=[0 1 2 3 4 5 6 7 8 9 10 11 12 13 14 15 16 17 18 19 20 21 22 23 24 25 26 ...
            27 28 29 30 31 32 33 34 35 36 37 38 39 40 41 42 43 44 45 46 47 48];
yaxis=[0.1 1.0 2.0 3.0 4.0 5.0 6.0 7.0 8.0 9.0 10.0];
        title('Select growth rate over time(nm/h)');
xlabel('time(h)');
ylabel('Growth rate(nm/h)');

[intime,inGR]=ginput();
for p=1:length(inGR)
ifinGR(p,1)<0
inGR(p,1)=0;
end;
end;
        intime(1,1)=0.2;
        intime(length(intime),1)=48;
sumGR=zeros(288:1);
sumGR(1,1)=inGR(1,1);

for x=2:length(intime);
timesteps(x-1)=floor((intime(x,1)*6))-floor((intime(x-1,1)*6));

startt(x-1)=floor(intime(x-1,1)*6);
dGR=inGR(x,1)-inGR(x-1,1);
```

```
dGRt=dGR/timesteps(x-1);

for z=1:timesteps(x-1)
sumGR(startt(x-1)+z,1)=sumGR(startt(x-1)+z-1,1)+dGRt;
ifsumGR(startt(x-1)+z,1)<0
sumGR(startt(x-1)+z,1)=0;
end;
end;
end;
end;
%%%%%%%%%%%%%%%%%%%%%%%%%%%%%%%%%%%%%%%%%%%%%%%%%%%%%%%%%%%%%%%%%%%%%%%%%%%%

%%%%%%%%%%%%%%% Input window for growth rate(Location dependent)%%%%%%%%%%%
interrupt3=menu('Press','Select growth rate(Location dependent)(nm/h)','Constant growth rate(Location dependent)');
if interrupt3==2
        interrupt3=true;
else
        interrupt3=false;
end

if interrupt3
%%%%%%%%%%%%%%% Input window for growth rate(Location dependent)%%%%%%%%%%%
        prompt = {'Enter constant growth rate(Location dependent)(nm/h)'};
dlg_title = 'Input';
num_lines = 1;
def = {'2'};
answerFR = inputdlg(prompt,dlg_title,num_lines,def);

%%%%%%%%%%%Conversion from cell to double%%%%%%%%%%%%%%%%%%%%%%%%%%%%%%%%%%
W = sprintf('%s*', answerFR{:});
inputGRL = sscanf(W, '%f*');   %Input values in double instead of cell
%%%%%%%%%%%%%%%%%%%%%%%%%%%%%%%%%%%%%%%%%%%%%%%%%%%%%%%%%%%%%%%%%%%%%%%%%%%%

else
        a=1;b=2;c=3;d=4;e=5;f=6;g=7;h=8;i=9;j=10;k=0;n=-1;y=Location:500:0;

figure(3);clf;

        plot(y,a,'-',y,b,'-',y,c,'-',y,d,'-',y,e,'-',y,f,'-',y,g,'-',y,h,'-',y,i,'-',y,j,'-',y,k,'-',y,n,'-');
xaxis=[0 1 2 3 4 5 6 7 8 9 10 11 12 13 14 15 16 17 18 19 20 21 22 23 24 25 26 ...
            27 28 29 30 31 32 33 34 35 36 37 38 39 40 41 42 43 44 45 46 47 48];
yaxis=[0.1 1.0 2.0 3.0 4.0 5.0 6.0 7.0 8.0 9.0 10.0];
        title('Select growth rate(Location dependent)(nm/h)')
```

```
xlabel('Location')
ylabel('growth rate(nm/h)')

[inLocation,inGRL]=ginput();
for p=1:length(inGRL)
ifinGRL(p,1)<0
inGRL(p,1)=0;
end;
end;
inLocation(1,1)=Location(1,1);
inLocation(length(inLocation),1)=0;
sumGRL=zeros(288:1);
sumGRL(1,1)=inGRL(1,1);
        intimes(1,1)=1;
dLocation=Location(1,2)-Location(1,1);
sumintimes(1,1)=intimes(1,1);

for r=2:length(inLocation)
for e=1:288
ifinLocation(r,1)>Location(1,e)
intimes(r,1)=e+1-sumintimes(r-1,1);
sumintimes(r,1)=sumintimes(r-1,1)+intimes(r,1);
end;
end;
end;
startt=zeros(length(inLocation):1);
for x=2:length(inLocation);
timesteps(x-1)=intimes(x,1);
startt(x-1,1)=sumintimes(x-1,1);
dGR=inGRL(x,1)-inGRL(x-1,1);
dGRL=dGR/timesteps(x-1);

for z=1:timesteps(x-1)
sumGRL(startt(x-1)+z,1)=sumGRL(startt(x-1)+z-1,1)+dGRL;
ifsumGRL(startt(x-1)+z,1)<0.01
sumGRL(startt(x-1)+z,1)=0;
end;
end;
end;
end;
%%%%%%%%%%%%%%%%%%%%%%%%%%%%%%%%%%%%%%%%%%%%%%%%%%%%%%%%%%%%%%%%%%%%%%%%%%%%%%

%%%%%%%% Input grafically the formation rate for the simulation time %%%%%%
interrupt4=menu('Press','Select formation rate over time(x10^8m^-3/h)','Constant formation rate over time');
if interrupt4==2
        interrupt4=true;
else
        interrupt4=false;
end

if interrupt4
```

```
%%%%%%%%%%%%%%% Input window for formation rate%%%%%%%%%%%%%%%%%%%%%%%%%%%%%%%%
        prompt = {'Enter constant formation rate over time(x10^8 m^-3/h):'};
dlg_title = 'Input';
num_lines = 1;
def = {'1'};
answerFR = inputdlg(prompt,dlg_title,num_lines,def);

%%%%%%%%%%%Conversion from cell to double%%%%%%%%%%%%%%%%%%%%%%%%%%%%%%%%%%%%
W = sprintf('%s*', answerFR{:});
inputFR = sscanf(W, '%f*');   %Input values in double instead of cell
%%%%%%%%%%%%%%%%%%%%%%%%%%%%%%%%%%%%%%%%%%%%%%%%%%%%%%%%%%%%%%%%%%%%%%%%%%%%%%%%

else
a=0;b=0;c=2e8;d=4e8;e=6e8;f=8e8;g=1e9;h=2e9;i=4e9;j=6e9;k=8e9;l=1e10;n=-1;y=0:0.1:48;
        a=0;b=0;c=1;d=2;e=3;f=4;g=5;h=6;i=7;j=8;k=9;l=10;n=-1;y=0:0.1:48;

figure(4);
clf;

xaxis=[0 1 2 3 4 5 6 7 8 9 10 11 12 13 14 15 16 17 18 19 20 21 22 23 24 25 26 ...
            27 28 29 30 31 32 33 34 35 36 37 38 39 40 41 42 43 44 45 46 47 48];
yaxis=[0 1 2 3 4 5 6 7 8 9 10 11 12 13 14 15 16 17 18 19 20 21 22 23 24 25];
        plot(y,a,'-',y,b,'-',y,c,'-',y,d,'-',y,e,'-',y,f,'-',y,g,'-',y,h,'-',y,i,'-',y,j,'-',y,k,'-',y,l,'-',y,n,'-');
        title('Select formation rate over time(x10^8 m^-3/h)')
xlabel('time(h)')
ylabel('formation rate(x10^8 m^-3/h)')

        [intime,inFR]=ginput();
for p=1:length(inFR)
ifinFR(p,1)<0
inFR(p,1)=0;
end;
end;
        intime(1,1)=0.2;
        intime(length(intime),1)=48;
sumFR=zeros(288:1);
sumFR(1,1)=inFR(1,1);

for x=2:length(intime);
timesteps(x-1)=floor((intime(x,1)*6))-floor((intime(x-1,1)*6));

startt(x-1)=floor(intime(x-1,1)*6);
dFR=inFR(x,1)-inFR(x-1,1);
```

```
dFRt=dFR/timesteps(x-1);

for z=1:timesteps(x-1)
sumFR(startt(x-1)+z,1)=sumFR(startt(x-1)+z-1,1)+dFRt;
ifsumFR(startt(x-1)+z,1)<0
sumFR(startt(x-1)+z,1)=0;
end;
end;
end;
end;
%%%%%%%%%%%%%%%%%%%%%%%%%%%%%%%%%%%%%%%%%%%%%%%%%%%%%%%%%%%%%%%%%%%%%%%%%%%

%%%%%%%%%%%%%%% Input window for formation rate(Location dependent)%%%%%%%%
interrupt5=menu('Press','Select formation rate(Location dependent)(x10^8 m^-3/h)','Constant formation rate(Location dependent)');
if interrupt5==2
        interrupt5=true;
else
        interrupt5=false;
end

if interrupt5
%%%%%%%%%%%%%%% Input window for formation rate%%%%%%%%%%%%%%%%%%%%%%%%%%%%
        prompt = {'Enter constant formation rate(Location dependent)(x10^8 m^-3/h):'};
dlg_title = 'Input';
num_lines = 1;
def = {'1'};
answerFR = inputdlg(prompt,dlg_title,num_lines,def);

%%%%%%%%%%%Conversion from cell to double%%%%%%%%%%%%%%%%%%%%%%%%%%%%%%%%%%
W = sprintf('%s*', answerFR{:});
inputFRL = sscanf(W, '%f*');   %Input values in double instead of cell
%%%%%%%%%%%%%%%%%%%%%%%%%%%%%%%%%%%%%%%%%%%%%%%%%%%%%%%%%%%%%%%%%%%%%%%%%%%

else
        a=0;b=0;c=1;d=2;e=3;f=4;g=5;h=6;i=7;j=8;k=9;l=10;n=-1;y=Location:500:0;

figure(5);
clf;

xaxis=[0 1 2 3 4 5 6 7 8 9 10 11 12 13 14 15 16 17 18 19 20 21 22 23 24 25 26 ...
            27 28 29 30 31 32 33 34 35 36 37 38 39 40 41 42 43 44 45 46 47 48];
yaxis=[0 1 2 3 4 5 6 7 8 9 10 11 12 13 14 15 16 17 18 19 20 21 22 23 24 25];
```

```
320.         plot(y,a,'-',y,b,'-',y,c,'-',y,d,'-',y,e,'-',y,f,'-',y,g,'-
     ',y,h,'-',y,i,'-',y,j,'-',y,k,'-',y,l,'-',y,n,'-');
321.         title('Select formation rate(Location dependent)(x10^8 m^-
     3/h)')
322. xlabel('Location')
323. ylabel('formation rate(x10^8 m^-3/h)')
324.
325.         [inLocation,inFRL]=ginput();
326. for p=1:length(inFRL)
327. ifinFRL(p,1)<0
328. inFRL(p,1)=0;
329. end;
330. end;
331. inLocation(1,1)=Location(1,1);
332. inLocation(length(inLocation),1)=0;
333. sumFRL=zeros(288:1);
334. sumFRL(1,1)=inFRL(1,1);
335.         intimes(1,1)=1;
336. dLocation=Location(1,2)-Location(1,1);
337. sumintimes(1,1)=intimes(1,1);
338.
339. for r=2:length(inLocation)
340. for e=1:288
341. ifinLocation(r,1)>Location(1,e)
342. intimes(r,1)=e+1-sumintimes(r-1,1);
343. sumintimes(r,1)=sumintimes(r-1,1)+intimes(r,1);
344. end;
345. end;
346. end;
347.
348. for x=2:length(inLocation);
349. timesteps(x-1)=intimes(x,1);
350. startt(x-1,1)=sumintimes(x-1,1);
351. dFR=inFRL(x,1)-inFRL(x-1,1);
352. dFRL=dFR/timesteps(x-1);
353.
354. for z=1:timesteps(x-1)
355. sumFRL(startt(x-1)+z,1)=sumFRL(startt(x-1)+z-1,1)+dFRL;
356. ifsumFRL(startt(x-1)+z,1)<0
357. sumFRL(startt(x-1)+z,1)=0;
358. end;
359. end;
360. end;
361. end;
362. %%%%%%%%%%%%%%%%%%%%%%%%%%%%%%%%%%%%%%%%%%%%%%%%%%%%%%%%%%%%%%%%%%%%%%%
     %%%%%%%%
363. %%%Input window for Initial particle number size distribution
     parameters%%%
364. prompt = {'Mode diameters 1(nm):','Mode diameters 2(nm):','Mode
     diameters 3(nm):','Mode diameters 4(nm):','Standard deviation mode
     1:','Standard deviation mode 2:','Standard deviation mode
     3:','Standard deviation mode 4:','Number concentration mode 1
     (#/cm^3):','Number concentration mode 2 (#/cm^3)','Number
```

```
    concentration mode 3 (#/cm^3):','Number concentration mode 4
    (#/cm^3):'};
365. dlg_title = 'Input';
366. num_lines = 1;
367. def =
    {'10','22','80','300','1.6','1.25','1.3','1.4','0.0','0e2','1e3','1e1
    '};
368. answer = inputdlg(prompt,dlg_title,num_lines,def);
369. %%%%%%%%%%%%%%%%%%%%%%%%%%%%%%%%%%%%%%%%%%%%%%%%%%%%%%%%%%%%%%%%%%%%%%%
    %%%%%
370.
371. tic
372.
373. %%%%%%%%%%Conversion from cell to
    double%%%%%%%%%%%%%%%%%%%%%%%%%%%%%%
374. S = sprintf('%s*', answer{:});
375. inputvalues = sscanf(S, '%f*');   %Input values in double instead
    of cell
376. %%%%%%%%%%%%%%%%%%%%%%%%%%%%%%%%%%%%%%%%%%%%%%%%%%%%%%%%%%%%%%%%%%%%%%%
    %%%%%
377.
378. %if interrupt1
379. for q=1:time_steps
380.         WS(q,1)=inputWS;        %Constant wind speed
381. end;
382. %else
383. %    WS=sumWS;                   %wind speed
384. %end;
385.
386. if interrupt2
387. for q=1:time_steps
388.         GRT(q,1)=inputGR;       %Constant wind speed
389. end;
390. else
391.     GRT=sumGR;                  %GR over time
392. end;
393.
394. if interrupt3
395. for q=1:time_steps
396.         GRL(q,1)=inputGRL;      %Constant GR Location dependent
397. end;
398. else
399.     GRL=sumGRL;
400. end;
401.
402. if interrupt4
403. for q=1:time_steps
404. JnuclT(q,1)=inputFR;    %Constant FR over time
405. end;
406. else
407. JnuclT=sumFR;               %FR over time
408. end;
409.
410. if interrupt5
```

```
411. for q=1:time_steps
412. JnuclL(q,1)=inputFRL;  %Constant FR location dependent
413. end;
414. else
415. JnuclL=sumFRL;             %FRlocationdependent
416. end;
417.
418.
419.
420. for box=1:1:time_steps % Runs for every box
421. disp(box);
422.
423.     Location(1,box)=0;        %The location of the measurement
     station
424. if box>=2
425. for t=box:-1:2
426.             Location(t-1)=Location(t)-WS(t,1)*600;   %The location
     of the box
427. end;
428. end;
429.
430. % BOX MODEL START HERE
431. %%%%%%%%%%%%%%%%%%%%%%%%%%%%%%%%%%%%%%%%%%%%%%%%%%%%%%%%%%%%%%%%%%%%%%%
     %%%%%%%%
432. % Initial particle number size distribution parameters:
433. dm1=inputvalues(1,1);           % mode diameters 1(nm)
434.     dm2=inputvalues(2,1);           % mode diameters 2(nm)
435.     dm3=inputvalues(3,1);           % mode diameters 3(nm)
436.     dm4=inputvalues(4,1);           % mode diameters 4(nm)
437.
438.     s1=inputvalues(5,1);            % standard deviation mode 1
439.     s2=inputvalues(6,1);            % standard deviation mode 2
440.     s3=inputvalues(7,1);            % standard deviation mode 3
441.     s4=inputvalues(8,1);            % standard deviation mode 4
442.
443.     N1=inputvalues(9,1);            % number concentration mode 1
     (#/cm^3)
444.     N2=inputvalues(10,1);           % number concentration mode 2
     (#/cm^3)
445.     N3=inputvalues(11,1);           % number concentration mode 3
     (#/cm^3)
446.     N4=inputvalues(12,1);           % number concentration mode 4
     (#/cm^3)
447.
448. %%%%%%%%%%%%%%%%%%%%%%%%%%%%%%%%%%%%%%%%%%%%%%%%%%%%%%%%%%%%%%%%%%%%%%%
     %%%%%%%%
449.
450. % constants:
451.
452. dt=simulation_time/time_steps;  % Model main time step in hours
453. dt_dynamics=1/60;               % Time step of coagulation, dry
     deposition and condensation within each main time step (h)
454. t=0;                           % Initial modeltime
```

```
455. t_day=0;                          % Initial time of the day (local
   time)
456.
457. % Initial diameters used to represent the size distribution:
458. binsnr=60; binsnr2=100;
459.     d=zeros(1,binsnr+1);
460.     d(1)=20;
461. for j=2:binsnr+1;
462.             d(j)=d(j-1)*1.0675;
463. end
464. vp=d.^3*pi/6;
465. dp=(d(1:length(d)-1)+d(2:length(d)))/2; % arithmetic mean diamter
   in each
466. dlogdp=log10(d(2:binsnr+1))-log10(d(1:binsnr));
467. ddp=d(2:binsnr+1)-d(1:binsnr);
468. Vp=(pi*(dp*10^-9).^3)/6;    % volume of singelparticel in each size
   bin  m^2.
469.
470.
471.     [dNdlogDp,f__]=DMPS_PSD(dp*10^-9,[dm1*10^-9,dm2*10^-9,dm3*10^-
   9,dm4*10^-9],[s1,s2,s3,s4],[N1*10^6,N2*10^6,N3*10^6,N4*10^6]);
472.
473. dNdlogDp_fixed=zeros(time_steps,binsnr2);
   PN=zeros(1,time_steps);PV=PN;time=PN;
474. N_bins=dNdlogDp.*dlogdp+0.1;
475. V_bins=N_bins.*Vp;      % dV (m^3/m^3)
476.
477.     T=293;                      % Initial temperature K
478. dens=1400; % kg/m^3
479. dyn_visc=1.8*10^-5*(T./298).^0.85;  % dynamicviscosity
480.
481.
482. for s=1:box % start of time steping
483.
484.         GR=GRT(s,1)*GRL(time_steps-box+s,1);
485. Jnucl=JnuclT(s,1)*JnuclL(time_steps-box+s,1)*10^8;
486. %['Box #', num2str(s)]  %See what box you are on
487.
488. % Add any type of time or spatial dependent nucleation rate,
   Bounday layer mixing height and growth rates etc.
489. %%%%%%%%%%%%%%%%%%%%%%%%%%%%%%%%%%%%%%%%%%%%%%%%%%%%%%%%%%%%%%%%%%%%%%%
   %%
490. %GR=sin(t_day/3.8-pi/2)+3;                    % Particle growth
   rate in (nm/h)
491. % if t>8 && t<13 || t>24+8 && t<24+13
492. % Jnucl=1E10;                                % Nucleation rate in
   particles m^-3 h^-1
493. % else
494. % Jnucl=0;
495. % end
496. %Jnucl=(sin(t_day/3.8-pi/2)+1)*1E10;         % Nucleation rate in
   particles m^-3 h^-1
497.
```

```
498.         MH=(sin(t_day/3.8-pi/2)*2+3)*200; % Bounday layer mixing
   height
499.         z0=0.8;                          % Roughness length (~0.8 for
   forest)
500.         z1=10;                           % Altitude within surface
   layer with wind speed observations
501. %wind_speed_z1=2;              % Wind speed at altitude z1 (m/s)
502. F_k_flux=0; %sin(t/3.8-pi/2)/10;  % Kinematic vertical heat flux in
   the surface layer (K m^-1 s^-1)
503. A_land_use=2;
504. a_land_use=1;
505. j_land_use=0.56;
506. forest_fraction=1;
507. %%%%%%%%%%%%%%%%%%%%%%%%%%%%%%%%%%%%%%%%%%%%%%%%%%%%%%%%%%%%%%%%%%%%%%%
   %%
508.
509. % Homogeneousnucleation:
510. ifJnucl>1 % Consider nucleation if the nucleation rate is larger
   than 0
511. binsnr=binsnr+1;
512. dp=[1.5,dp]; % Add one new size bin at 1.5 nm in diameter
513. N_bins=[Jnucl*dt,N_bins]; % add new particles to the smallest size
   bin
514. end
515.
516. % Coagulationalgorithm
517. for j=1:round(dt/dt_dynamics)
518. %Coagulation
519. N_bins=coagulation(N_bins,dp,dt_dynamics,T,dens,dyn_visc);
520.
521. %Condensation:
522. dp=dp+(GR*dt_dynamics);
523.
524. %Dry deposition
525.
   vd=dry_deposition_velocity(dp,z0,WS(s,1),T,F_k_flux,MH,z1,A_land_use,
   a_land_use,j_land_use,forest_fraction,dens); % m/h
526. N_bins=N_bins.*exp(-vd*dt_dynamics/MH);
527. Vp=(dp*10^-9).^3*pi/6;
528. V_bins=N_bins.*Vp;
529. end
530.
531.         t=t+dt; % update time (h)
532. t_day=t_day+dt; % time of the day along the trajectory
533. ift_day>24
534. t_day=0;
535. end
536. % Converts moving size structure particle number size distribution
   to fixed
537. % diameter grid:
538. d_fixed=zeros(1,binsnr2+1);
539. d_fixed(1)=1.5;
540. for j=2:binsnr2+1;
541. d_fixed(j)=d_fixed(j-1)*1.0675;
```

```
end
vp_fixed=d_fixed.^3*pi/6;
        dp_fixed=(d_fixed(1:length(d_fixed)-1)+d_fixed(2:length(d_fixed)))/2; % arithmetic mean diamter in each
dlogDp_fixed=log10(d_fixed(2:binsnr2+1))-log10(d_fixed(1:binsnr2));

N_bins_fixed=zeros(1,binsnr2+1);
Vp=dp.^3*pi/6;
for j=1:length(dp)-1
for ii=1:length(d_fixed)-1;
ifVp(j)>=vp_fixed(ii) &&Vp(j)<vp_fixed(ii+1)
% Splitting parameters to convert full moving diameter grid back to full
% stationarygrid.
                    r1=(vp_fixed(ii+1)-Vp(j))./(vp_fixed(ii+1)-vp_fixed(ii)); % Fraction of particles in size bin j
                    r2=1-r1; % Fraction of particles in next size bin (j+1)
N_bins_fixed(ii)=N_bins_fixed(ii)+r1*N_bins(j);
N_bins_fixed(ii+1)=N_bins_fixed(ii+1)+r2*N_bins(j);
end
end
end
dNdlogDp_fixed(s,:)=N_bins_fixed(1:binsnr2)./dlogDp_fixed*10^-6;
        PN(s)=sum(N_bins)*10^-6;
        PV(s)=sum(V_bins)*10^12;
time(s)=t-dt/2;
end

saved_box(box,:)=dNdlogDp_fixed(box,:);
end;

time_vector=0:10/60/24:1-10/60/24;
time_vector=time_vector+1;
size_vector=[0 0 dp_fixed]*1e-9;
N_vector=sum(saved_box')*dlogDp_fixed(1);
save_matrix1=[size_vector
time_vector' N_vector(1:144)' saved_box(1:144,:)];
save_matrix2=[size_vector
time_vector' N_vector(145:end)' saved_box(145:end,:)];
savefile1='data100101.sum';
save(savefile1,'save_matrix1','-ascii','-tabs','-double');
savefile2='data100102.sum';
save(savefile2,'save_matrix1','-ascii','-tabs','-double');

figure(6)
colormap(jet(250));
pcolor(time,log10(dp_fixed),(saved_box.^0.15)')
shadinginterp
yaxis=[log10(1) log10(2) log10(10) log10(20) log10(30) log10(40) log10(50) log10(60) log10(70) log10(80) log10(90) log10(100) log10(200) log10(300)...
    log10(400) log10(500) log10(600) log10(700) log10(800) log10(900) log10(1000)];
```

```
set(gca,'yticklabelmode','manual')
set(gca,'ytick',yaxis,'yticklabel',{[],2,10,[],[],[],[],[],[], ...
      [],[],100,[],[],[],500,[],[],[],[],[]})
set(gca,'fontsize',10);
ylabel('Diameter (nm)','fontsize',10);
xlabel('time (h)')
H=colorbar;
set(H,'fontsize',10,'YTick',[10^0.15,100^0.15,1000^0.15,10000^0.15,
100000^0.15],'YTickLabel',[10,100,1000,10000,100000])
title('Particle number size distribution (cm^-^3)')

toc
```

8.2 Coagulation code

```
functionN_bins=coagulation(N_bins,dp,dt,T,dens,dyn_visc)

% Coagulation coefficients for coagulation between each particle
size:
l=6.53*10^-8;               % Gas mean free path in m
k_b=1.38*10^-23;            % Bolzmann'sconstant
u=dyn_visc;                 % Dynamicviscosity

Vp=(4*pi*((dp/2)*10^-9).^3)./3; % volume of singelparticel in each
size bin m^3.

C=1+(2*l./(dp.*10^-9)).*(1.257+0.4.*exp(-1.1./(2*l./(dp.*10^-9))));
% Cunninghams correction factor

D=C.*k_b.*T./(3*pi*u.*dp.*10^-9);          % Diffusivitys for the
different particle sizes m^2/s

m=(dens.*pi.*(dp*10^-9).^3)/6;  % mass of particles
c=(8*k_b*T./(pi*m)).^0.5; % speed of particles
l=8*D./(pi*c); % mean free path
g=(1./(3*(dp*10^-9).*l)).*((dp*10^-9+l).^3-((dp*10^-
9).^2+l.^2).^(3/2))-dp*10^-9;
K=zeros(length(dp),length(dp));
for n=1:length(dp)
    beta=((dp*10^-9+dp(n)*10^-9)./(dp*10^-9+dp(n)*10^-
9+2*(g.^2+g(n).^2).^0.5)+8*(D+D(n))./(((c.^2+c(n).^2).^0.5).*(dp*10^-
9+dp(n)*10^-9))).^-1; % Fuchs correction factor from Seinfeld and
Pandis, 2006
    K(n,:)=2*pi*beta.*(dp*10^-9*D(n)+dp*10^-9.*D+dp(n)*10^-
9*D+dp(n)*10^-9*D(n)); % coagulation rates between two particles of
all size combinations  (m^3/s)
end

%%%%%%%%%%%%%%%%%%%%%%%%%%%%%%%%%%%%%%%%%%%%%%%%%%%%%%%%%%%%%%%%%%%%%%%%
%%
dNdt=zeros(1,length(dp)+1);
dp_max=dp(length(dp))*dp(length(dp))/dp(length(dp)-1);
Vp(length(dp)+1)=(pi*dp_max^3)/6;

```

```
% Coagulation source:
for j=1:length(dp)
for k=1:j
if k==j
            a=0.5; % self-coagulation
else
            a=1;
end
Vp_coag=Vp(k)+Vp(j); % Volume of new particles formed by coagulation
fori=j:length(dp);
ifVp_coag>=Vp(i) &&Vp_coag<Vp(i+1)

% If i=j some of the particles will stay in the same size bin as
before.
% This is anyway treated as a source into the old size bin because
it is assumed
% that all particles are lost due to coagulation in that same size
bin
% below

% Splitting parameters:
r1=(Vp(i+1)-Vp_coag)/(Vp(i+1)-Vp(i)); % Fraction of particles in
size bin i
r2=1-r1; % Fraction of particles in next size bin (i+1)

Koag_source=a*K(k,j)*N_bins(j)*N_bins(k); % (m^3/s)
dNdt(i)=dNdt(i)+r1*Koag_source; % (#/m^3 s)
dNdt(i+1)=dNdt(i+1)+r2*Koag_source; % (#/m^3 s)
end
end
end
end

% Coagulation sink included:
Koag_sink=dp*0;
for j=1:length(dp)
for k=1:length(dp)
Koag_sink(k)=K(j,k)*N_bins(k).*N_bins(j); % (m^3/s)
end
Koag_sinktot=sum(Koag_sink); % prevent negative concentrations due
to too long time step
dNdt(j)=dNdt(j)-Koag_sinktot;
end

N_bins=N_bins+dNdt(1:length(dp))*dt*3600; % New particle
concentration in each size bin
N_bins(N_bins<0.1)=0.1;
```

8.2 Dry deposition velocity code

```
% m-file that calculates the dry deposition velosity for each size
bin
```

```
function vd=dry_deposition_velocity(dp_wet,z0,wind_speed_z1,T,F_flux,H,z1,A,a,j,forest_fraction,dens)
% Aerodynamicresistance
k=0.41; % von Karman constant
u=k.*wind_speed_z1./log(z1./z0); % friction velocity
g=9.81; % gravitation constant
L=-T.*u.^3./(k*g.*F_flux'); % Monin-Obukhov length

zr=0.1*H; % approximated height of the surface layer
ifzr>100;
zr=100;
end

Rf0=z0./L; % Richards number ground
Rfr=zr./L; % Richards number top of the surface layer


for f=1:length(Rfr)
if Rf0(f)>=1/15   % limits how stable or unstable the atmospher can be before the teorydose not work any more
Rf0(f)=1/15;
end
ifRfr(f)>=1/15
Rfr(f)=1/15;
end
end

y0=(1-15*Rf0).^0.25;
yr=(1-15*Rfr).^0.25;


ifRfr>=0;
ra=(1/(k*u))*(log(zr/z0)+4.7*(Rfr-Rf0)); % aerodynamic resistance stable atmosphere
else
ra=(1/(k*u))*(log(zr/z0)+log((y0^2+1)*(y0+1)^2/((yr^2+1)*(yr+1)^2))+2*(atan(yr)-atan(y0))); % aerodynamicresistanceunstableatmosphere
end

% Quasi-laminarresistance
Dp=dp_wet*10^-9; % particle diameters for each size bins after water uptake
vd=zeros(1,length(Dp));
for i=1:length(Dp)

R1=1; % all particles stick to the surface when contact if R1=1

v=1.34*10^-5; % Pa s kinematic viscosity of air at T=273.15 K
mu=1.8*10^-5.*(T./298).^0.85; % dynamicviscosity
k_b=1.381*10^-23; % Bolzmannconstant
q=0.0651*10^-6; % meanfreepath
```

```
Cc=1+(2*q/Dp(i))*(1.257+0.4*exp(-1.1*Dp(i)/(2*q))); % slip correction factor
D=k_b.*T.*Cc./(3*pi*mu*Dp(i)); % Brownian diffusivity
Sc=v./D; % Schmidt number
vs=dens*Dp(i)^2*g*Cc./(18.*mu); % sedimentation velosity
St=vs.*u./(g*A); % Stokes number
ifforest_fraction>0
rb=1./(3.*u.*R1.*(Sc.^-j+((St./(a+St)).^2+0.5*(Dp(i)/A).^2)));
else
rb=(k*wind_speed_z1)/u^2*(1/(Sc^-(1/2)+10^(-3/St))); % Quasi-laminar resistance over ocean (Slinn and Slinn, 1980)
end

vd(i)=3600*(1./(ra+rb+ra.*rb.*vs)+vs)'; % m/h
end
```

8.2 DMPS_PSD code

```
function [NDist_,NDist] = DMPS_PSD(Dp,Dpg,sig,Ntot)
%-------------------------------------------------------------------------%
% DMPS_PSD is a subroutine that generates the particle size distribution
% from the multi-lognormal parameters.
%   Dp = is the particle size grid for the distribution to be evaluated
%   Dpg = geometricparticle diameters
%   sig = geometric standard deviations
%   Ntot = total concentration in each mode
%
% The result is returned as follows:
%   NDist_ = is the overall particle size distribtution
%   NDist  = is a matrix that contains the particle size distribution of
%            the modes seperately
%
%   Tareq Hussein, April 2003.
%
%
%-------------------------------------------------------------------------%
mm = length(Dpg);
fori   = 1:1:mm;
NDist(i,:) = ( Ntot(i) / 2.506628 / log10(sig(i))) .* ...       % sqrt(2*pi) = 2.506628
exp( - ( ( log10(Dp) - log10(Dpg(i)) ) .^2 ) ./ ( 2 * log10(sig(i))^2 ) );
end
if mm ~= 1
NDist_ = sum(NDist);
end
%-------------------------------------------------------------------------%
```